ELECTROMAGNETIC BAND GAP (EBG) FOR MICROSTRIP ANTENNA DESIGN

AINOR KHALIAH BINTI MOHD ISA

A thesis submitted in fulfillment of the
requirement for the award of the degree of
Master of Engineering
(Electrical-Electronics of Telecommunication)

Faculty of Electrical Engineering
Universiti Teknologi Malaysia

MAY 2007

To my beloved mother and father

ACKNOWLEDGEMENT

In the name of Allah, the Most Beneficent and Most Merciful, Who has created the mankind with knowledge, wisdom and power.

First and foremost, I would like to express my deep and sincere gratitude to my supervisor, Dr Mohamad Kamal bin Abdul Rahim. His wide knowledge and his logical way of thinking have been of great value for me. His understanding, encouraging and personal guidance have provided a good basis for the present project.

I wish to express my warm and sincere thanks to Mr. Thelaha bin Masri for the constant help and knowledge contribution to ensure the success of the project. I would also like to thank all of my friend for the generous support throughout the semester, Zuhanis, Muza, Bambang, KB, Suria and Farah.

I cannot end without thanking my family and my love one, on whose constant encouragement and love I have relied throughout my research in completing this project. May God bless each and every one of you.

ABSTRACT

Microstrip patch antennas became very popular in mobile and radio wireless communication. This is because of ease of analysis and fabrication, and their attractive radiation characteristics. However, they have some drawbacks of low efficiency, narrow bandwidth and surface wave losses. In order to overcome the limitations of microstrip antennas such as narrow bandwidth (< 5%), lower gain (-6 dB), excitation of surface waves etc, a new solution method; using electromagnetic bandgap (EBG) materials, as substrates has attracted increasing attention. Unlike other methods, this new method utilizes the inherent properties of dielectric materials to enhance microstrip antenna performance. These periodic structures have the unique property of preventing the propagation of electromagnetic waves for specific frequencies and directions which are defined by the shape, size, symmetry, and the material used in their construction. Some EBG structures include drilled holes in dielectrics, patterns etched in the ground plane, and metallic patches placed around microstrip structures. The aim of this project are to design, simulate and fabricate the new EBG structure operating at 2.4GHz frequency and study the performance of the rectangular microstrip antenna with and without EBG structure. Those designs were simulated with Microwave Office software and tested with the Network Analyzer. Both, simulated and measured data were compared and contrasted.

ABSTRAK

Antena mikrojalur menjadi semakin popular dalam bidang telekomunikasi tanpa wayar bergerak. Ini disebabkan kemudahan dalam analisis, fibrikasi, dan mempunyai karakter radiasi yang menarik. Walaubagaimana pun, ianya mempunyai beberapa kelemahan seperti kecekapan yang rendah, jalurlebar yang sempit dan kehilangan gelombang permukaan. Untuk mengatasi masalah ini, satu penyelesaian baru, iaitu penggunaan bahan jalurcelah elektromagnet (EBG) boleh digunakan. Berbanding cara yang lain, cara in menggunakan sifat semulajadi bahan dielektrik untuk menambahkan keupayaan antenna mikrojalur. Struktur yang berkala ini mempunyai sifat yang unik iaitu menghalang perambatan gelombang elektromagnet untuk frekuensi dan arah yang tertentu berdasarkan bentuk, saiz, dan bahan yang digunakan untuk membinanya. Sesetengah struktur EBG ini termasuklah menebuk lubang pada dielektrik, mengukir corak pada permukaan bawah dan tampalan logam di sekeliling struktur mikrojalur. Tujuan projek ini ialah untuk merekabentuk, simulasi and fibrikasi struktur EBG yang baru dan beroperasi pada frekuensi 2.4GHz dan mengkaji kebolehan antenna mikrojalur dan antenna mikrojalur dengan jalurcelah elektromagnet. Kesemua rekaan ini disimulasi menggunakan perisian Microwave Office dan diuji menggunakan Network Analyzer. Keputusan kedua-dua rekaan ini dibanding antara satu sama lain.

TABLE OF CONTENTS

CHAPTER	TITLE	PAGE
	TITLE	i
	DECLARATION	ii
	DEDICATION	iii
	ACKNOWLEDGEMENT	iv
	ABSTRACT	v
	ABSTRAK	vi
	TABLE OF CONTENTS	vii
	LIST OF TABLES	xi
	LIST OF FIGURES	xii
	LIST OF SYMBOLS	xvi

CHAPTER 1 INTRODUCTION

1.1 Introduction 1
1.2 Objectives 2
1.3 Scope of work 2
1.4 Outline of the thesis 2
1.5 Summary 3

CHAPTER 2 MICROSTRIP PATCH ANTENNA

2.1 Introduction 4
2.2 Basic characteristic 5
2.3 Microstrip antenna properties 6
  2.3.1 Polarization 6
  2.3.2 Radiation Pattern 7
  2.3.3 Half Power Beamwidth (HPBW) 8
  2.3.4 Gain 9
  2.3.5 Voltage Standing Wave Ratio (VSWR) 10
  2.3.6 Bandwidth 11
2.4 Feeding Techniques 11
2.5 Methods of analysis 13
2.6 Summary 13

CHAPTER 3 ELECTROMAGNETIC BAND GAP (EBG)

3.1 Introduction 14
3.2 Formation of surface waves (surface Plasmon) 15
3.3 Perforated EBG structure 16
3.4 Metallodielectric EBG structure 19
3.5 Applications of electromagnetic band gap (EBG) structure. 20
  3.5.1 A multi-period EBG structure for microstrip antenna 20
  3.5.2 Wideband microstrip patch antenna with EBG substrate 25
3.6 Summary 31

CHAPTER 4 DESIGN METHODOLOGY

4.1 Conventional Microstrip antenna design 32
  4.1.1 Theoretical design 32
  4.1.2 Design Specifications 34
4.2 Electromagnetic band gap (EBG) structure design 35
  4.2.1 Design Specification 36
4.3 Microstrip antenna with EBG structure 37
4.4 Simulation 37

4.5 Fabrication 38
  4.5.1 Generate mask on transparency 38
  4.5.2 Photo exposure process 38
  4.5.3 Etching in developer solution 39
  4.5.4 Etching in Ferric Chloride 39
  4.5.5 Soldering the probe 39
4.6 Testing (Measurement) 43
4.7 Summary 43

CHAPTER 5 SIMULATION AND MEASUREMENT RESULTS
5.1 Conventional Microstrip antenna 44
5.2 Electromagnetic band gap (EBG) structure 48
  5.2.1 Effect of the vias locations 52
  5.2.2 Effect of the separation (gap) 53
5.3 Microstrip antenna with EBG structure 55
5.4 Summary 58
CHAPTER 6 CONCLUSIONS AND SUGGESTIONS
6.1 Conclusion 59
6.2 Suggestion for future works 60
REFERENCES 61
APPENDIX A 64

LIST OF TABLES

TABLE NO. TITLE PAGE

2.1 Conversion Table for SWR 10

4.1 Design parameters of microstrip antenna 34

5.1 Comparison between conventional microstrip antenna and microstrip antenna with EBG structure 58

LIST OF FIGURES

FIGURE NO. TITLE PAGE

2.1 Typical geometry of a microstrip antenna 5

2.2 Types of antenna polarization 7

2.3 Radiation pattern of a generic directional antenna 8

2.4 Half power beamwidth 9

2.5 Feeding Methods 12

3.1 Field lines radiating from a patch antenna; illustrates the formation of surface waves 16

3.2 Technique used to fabricate the first 3D PC structure, the Yablonovite 17

3.3 2D photonic crystal structure patterned with a triangular crystal lattice; the crystal lattice is of cylindrical air posts in a high dielectric substrate. 17

3.4 Illustration of a patch designed on a photonic crystal substrate; defect introduced in the area under the patch 18

3.5 Cross section views of the patches of the conventional and sandwiched EBG substrates 21

3.6 Schematic of the single and multi period EBG structure sandwiched between the patch antenna and ground plane. 22

3.7 Simulated (solid line) and measured (dotted line) input beam loss (S11) for conventional and two antennas on the sandwiched EBG structure. 23

3.8 Simulated (solid line) and measured (dotted line) radiation patterns for conventional patch and two patches on the single period and multiperiod EBG structure 24

3.9 Geometry of a two layer EBG structure 26

3.10 Magnitude of RCS vs. frequency on a two layer EBG structure with $\varepsilon_r = 2.5$, $h_1=h_2=1.59$mm, wave incident horizontally with vertical polarization. 26

3.11 Radiation patterns of the reference antenna with L=9mm, W= 4mm, $\varepsilon_r = 2.5$, h=1.59mm, L_f= 0.8mm, ground plane: 60mm by 60mm (a) Front radiation (b) Back radiation 27

3.12 E and H plane radiation patterns of a single layer EBG antenna with L=9mm, W= 4mm, $\varepsilon_r = 2.5$, h=1.59mm, L_f= 0.8mm, ground plane: 60mm by 60mm at 9.87GHz (a) Front radiation (b) Back radiation 28

3.13 Geometry of the two layer EBG antenna with L=9mm, W =4mm, $\varepsilon_r = 2.5$, $h_1=h_2=1.59$mm, L_f =2.1mm, X_0 =12mm, Y_0 =8.3mm, EBG: 8mm by 8mm and 7.8mm by 8mm, spacing 0.2mm and 0.1mm, ground plane:60mm by 60mm. 29

3.14 The S11 of the optimized two layer EBG antenna of Figure 3.13 30

3.15 E and H plane radiation patterns of the optimized two layer EBG antenna of Figure 3.13 at 11.36GHz (a) Front radiation (b) Back radiation 31

4.1 EM structure for conventional rectangular microstrip antenna 35

4.2 EM structure for EBG structure 37

4.3 Circuit pattern on transparency 40

4.4 Photo exposure machine 40

4.5 Etching in developer solution 40

4.6 Etching in ferric chloride 41

4.7 Soldering process 41

4.8 Flowchart of the fabrication process 42
4.9 Marconi Scalar Analyzer 6204 43
5.1 EM structure with the calculated value of W, L and port position 45
5.2 Fabricated structure of microstrip antenna 45
5.3 3D layout of the conventional rectangular patch antenna with the coaxial feed 46
5.4 Return Loss for conventional rectangular patch antenna 47
5.5 Maximum radiation at 0°, gain = 5.58dB for conventional rectangular patch antenna 48
5.6 EM structure for the EBG 49
5.7 Fabricated view of EBG structure 49
5.8 3D layout of the EBG structure with the transmission line analysis method 50
5.9 S21 parameter for the EBG structure 51
5.10 Comparison of S21 parameters between simulation and measurement values of the EBG structure 51
5.11 Different location of the vias in the EBG structure 52
5.12 Comparison of S21 for the different location of vias 53
5.13 Different separation (gap) of the EBG structure 54
5.14 Comparison of S21 parameters for different separation gap of EBG structure. 55
5.15 EM structure of microstrip antenna with EBG structure 56
5.16 3D layout of the microstrip antenna with EBG structure 57
5.17 Maximum radiation at 0°, gain = 7.689dB for microstrip antenna with EBG structure 57

LIST OF SYMBOLS

mm - millimeter

dB - decibel

Hz - hertz

K - kilo

D,d - diameter

H - height

L - length

W - width

Γ - reflection coefficient

Z_0 - characteristic impedance

λo - free-space wavelength

ε_r - dielectric constant of the substrate

h - patch thickness

c - speed of light $3x\ 10^{-8}$ m/s

CHAPTER 1

INTRODUCTION

1.1 Introduction

Microstrip patch antennas have been an attractive choice in mobile and radio wireless communication. This is because they have advantages such as low profile, conformal, low cost and robust. However, at the same time they have disadvantages of low efficiency, narrow bandwidth and surface wave losses.

Recently, there has been considerable research effort in the electromagnetic band gap (EBG) structure for antenna application to suppress the surface wave and improve the radiation performance of the antenna.

In this project, it is proposed that the microstrip antenna having the EBG structure, which is placed around the patch antenna. The proposed design is evaluated using the Microwave Office and the effectiveness of the design is compared with the conventional microstrip antenna.

1.2 Objectives

The objectives of this project are to design, simulate and fabricate the new EBG structure operating at 2.4GHz frequency and study the performance of the rectangular microstrip antenna with and without EBG structure.

1.3 Scope of work

The scopes of work of this project are to study the basic electromagnetic band gap (EBG) properties from several published papers and books, design a conventional rectangular microstrip antenna and the new EBG structure operating at 2.4GHz frequency.

These designs are simulated using Microwave Office software. The designs were then etched on FR4 substrate with dielectric constant of 4.5 and height of 1.6 mm. Network Analyzer was used to measure the designs. Both simulated and measured data are compared and contrasted.

1.4 Outline of the Thesis

The thesis consists of six chapters and the overview of all the chapters are as follows:

Chapter 1:	This chapter provides a brief introduction on the background, the objectives of the project and scope of work involved in accomplishing the project.
Chapter 2:	A technical description of microstrip antenna focusing on basis characteristics and typical excitation (feeding) methods, and

concludes with an analytical model of the patch were discussed in this chapter.

Chapter 3:	Literature review of electromagnetic bang gap (EBG) is describes in this chapter. This chapter focuses on the underlying principles of electromagnetic band gap (EBG) and their associate properties.
Chapter 4:	This chapter gives an overview of the antenna design methodology with the fundamental process in the design, simulate, fabricate and testing (measurement) procedures.
Chapter 5:	Chapter 5 describes the simulation and measurement results obtained from the described methodology.
Chapter 6:	A final conclusions is made in chapter 6 based on the outcome of the project, followed by the recommendations for the future work.

1.5 Summary

This chapter provides the introduction for the project. Its cover the objectives, scope of work and the flow of this thesis. This chapter is the major part of the thesis because its summaries the whole process.

CHAPTER 2

MICROSTRIP PATCH ANTENNA

2.1 Introduction

Microstrip antennas became very popular in the 1970s primarily for space borne applications. Today they are used for government and commercial applications. Through decades of research, it was identified that the performance and operation of microstrip antenna is driven mainly by the geometry of the printed patch and the material characteristics of the substrate onto which the antenna is printed. The microstrip antenna became very popular because of ease of analysis and fabrication, and their attractive radiation characteristics. The microstrip antenna offers low-profile, conformable to planar and non-planar surfaces, simple and inexpensive to fabricate using modern printed-circuit technology, mechanically robust when mounted on rigid surfaces and very versatile in terms of resonant frequency, polarization, patterns and impedance. Major disadvantages of microstrip antenna are their low efficiency, low power, poor polarization purity, poor scan performance, very narrow frequency bandwidth and existence of surface waves. [1]

2.2 Basic Microstrip antenna

The conventional microstrip antenna consists of a pair of parallel conducting layers separating a dielectric medium, referred to as the substrate as shown in Figure 2.1.

In this configuration, the upper conducting layer or patch is the source of radiation where electromagnetic energy fringes off the edges of the patch and into the substrate. The lower conducting layer acts as a perfectly reflecting ground plane, bouncing energy back through the substrate and into free space.

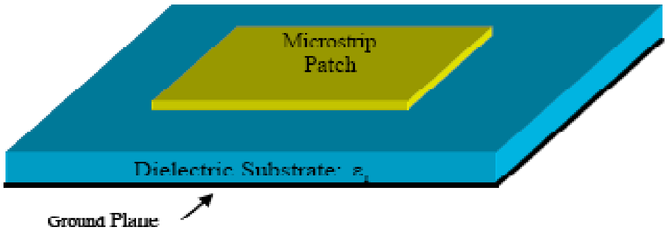

Figure 2.1: Typical geometry of a microstrip antenna

There are numerous substrates that can be used for design of microstrip antennas, and their dielectric constants are usually in the range of $2.2 \leq \varepsilon r \leq 12$ for operation at frequencies ranging from 1 to 100GHz.

The ones that are most desirable for antenna performance are thick substrates whose dielectric constant is in the lower end of the range because they provide better efficiency, larger bandwidth, loosely bound fields for radiation into space, but at the expense of larger element size. [2] Thin substrates with higher dielectric constants are desirable for microwave circuitry because they required tightly bound fields to minimize undesirable radiation and coupling, and lead to smaller element sizes; however, because of their greater losses, they are less efficient and have relatively smaller bandwidth. [2]

2.3 Microstrip antenna properties

To describe the performance of an antenna, definitions of various parameters are necessary. Some of the parameters are interrelated and not at all of them need to be specified for complete description of the antenna performance.

2.3.1 Polarization

Polarization of an antenna in a given direction is defined as the polarization of the wave transmitted (radiated) by the antenna. Polarization of the radiated wave is defined as property of an electromagnetic wave describing the time varying direction and relative magnitude of the electric field vector. Polarization may be classified as linear, circular, or elliptical as shown in Figure 2.2.

Polarization also can be defined as the orientation of the electric field vector component of the electromagnetic field. In line-of-sight communications it is important that transmitting and receiving antennas have the same polarization (horizontal, vertical or circular). In non-line-of-sight the received signal undergoes multiple reflections which change the wave polarization randomly.

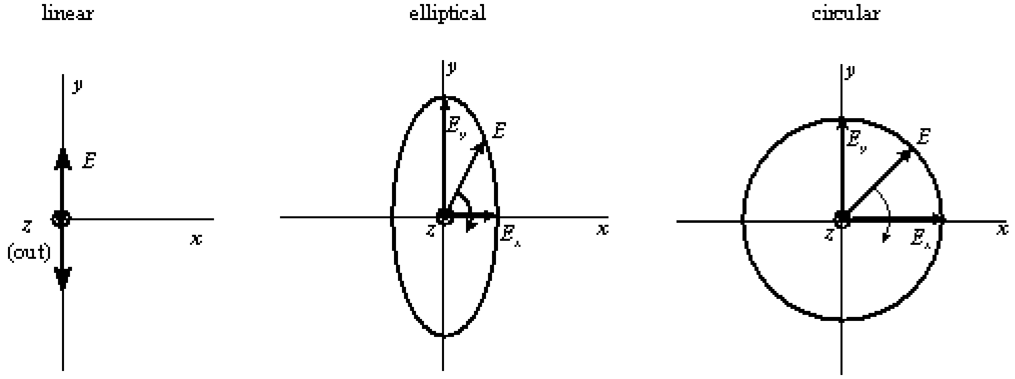

E = electrical field vector

Figure 2.2: Types of antenna polarization

2.3.2 Radiation Pattern

An antenna radiation pattern or antenna pattern is defined as “a mathematical function or a graphical representation of the radiation properties of the antenna as a function of space coordinates. In most cases, the radiation pattern is determined in the far-field region and is represented as a function of the directional coordinates. Radiation properties include power flux density, radiation intensity, field strength, directivity phase or polarization. The radiation pattern could be divided into:

i. Main lobes

This is the radiation lobe containing the direction of maximum radiation.

ii. Side lobes

These are the minor lobes adjacent to the main lobe and are separated by various nulls. Side lobes are generally the largest among the minor lobes.

iii. Back Lobes

This is the minor lobe diametrically opposite the main lobe.

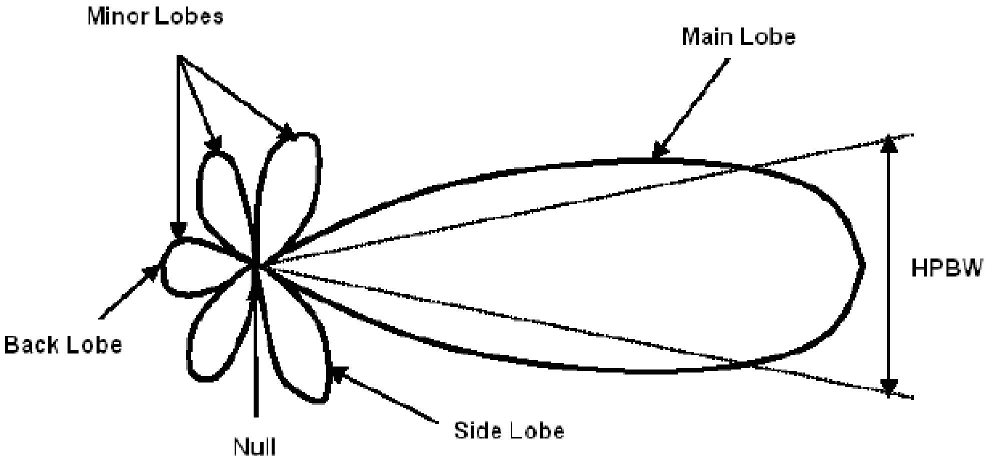

Figure 2.3: Radiation pattern of a generic directional antenna.

2.3.3 Half Power Beamwidth (HPBW)

The half power beamwidth is defined as: “In a plane containing the direction of the maximum of a beam, the angle between the two directions in which the radiation intensity is one half the maximum value of the beam.” Often the term beamwidth is used to describe the angle between any two points on the pattern, such as the angle between the 10dB points. In this case the specific points on the pattern must be described to avoid confusion. However the term beamwidth by itself is usually reversed to describe the 3dB beamwidth as shown in Figure 2.4.

The beamwidth of the antenna is a very important figure-of-merit, and it often used to as a tradeoff between it and the sidelobe level. In addition, the beamwidth of the antenna is also used to describe the resolution capabilities of the antenna to distinguish between two adjacent radiating sources or radar targets.

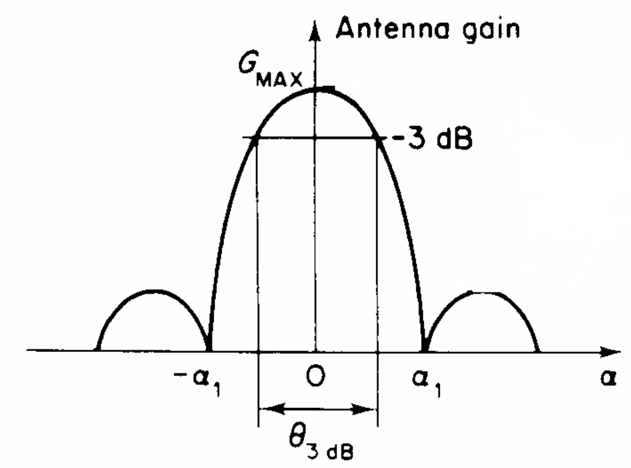

Figure 2.4: Half power beamwidth

2.3.4 Gain

Antenna gain is a measure of directivity properties and the efficiency of the antenna. It is defined as the ratio of the radiation intensity in the peak intensity direction to the intensity that would be obtained if the power accepted by the antenna were radiated isotropically. The difference between the antenna gain and the directivity is that the antenna efficiency is taken into account in the former parameter. Antenna gain is measured in dBi, i.e. decibels relative to isotropic antenna. Figure 2.5 show the type of antenna gain.

2.3.5 Voltage Standing Wave Ratio (VSWR)

Voltage Standing Wave Ratio is the ratio of the maximum to minimum voltage on the antenna feeding line. Standing wave pattern is created on the feeding line when the impedance match is not perfect and a fraction of the power put into antenna is reflected back and not radiated. For perfectly impedance matched antenna the VSWR is 1:1.

VWSR causes return loss or loss of forward energy through a system. Typical value of VSWR would be 1.5:1, where the two first numbers relate the ratio of impedance mismatch against a perfect impedance match and the second number is always 1, representing the perfect match. This impedance mismatch will reduce system efficiency. Table 2.1 shows the conversion for SWR.

Table 2.1: Conversion Table for SWR

Power reflected (%)	Power transmitted into comp. (%)	Return Loss (dB)	SWR	Reflection coefficient
1	99	20	1.25	0.10
5	95	13	1.58	0.22
10	90	10	1.95	0.32
20	50	3	5.80	0.71

2.3.6 Bandwidth

The bandwidth of an antenna is defined as the range of frequencies within which the performance of the antenna, with respect to some characteristic, conforms to a specified standard. The bandwidth can be considered to be the range of frequencies, on either side of a center frequency (usually the resonance frequency for a dipole), where the antenna characteristic (such as input impedance, pattern, beamwidth, polarization, side lobe level, gain, beam direction, radiation efficiency) are within an acceptable value of those at the center frequency.

2.4 Feeding Techniques

There are several techniques available to feed or transmit electromagnetic energy to a microstrip antenna. The most popular methods are the microstrip transmission line, coaxial probe, aperture coupling and proximity coupling. [1] Figure 2.5 illustrates each of these configurations. In each of the equivalent circuits, an RLC corresponds to loss associate with the conductors (ground plane and patch) and substrate (loss tangent).

The simplest feeding methods to realize are those of the coaxial probe and microstrip transmission line. Both approaches utilize direct contact with the patch to induce excitation. The point of excitation (contact point) is adjustable, is enabling the designer to control the impedance match between feed and antenna, polarization, mode of operation and excitation frequency.

Generally, for direct contact feed, the best impedance match is obtained when the contact point is off-centered. This produces asymmetries in the patch excitation which generate higher order modes. [3] These higher order modes induce a cross-polarized component in the principal plane antenna patterns, which draw power from the dominant TM010 mode and results in degradation of the antenna’s main beam. Therefore, oftentimes, a trial and error approach is used to obtain the optimum match for the direct contact feeds.

Another disadvantage of the direct contact feeds is that they are inherently narrowband devices. These feeds, whether coaxial or microstrip, are matched to specific impedances for a select range of frequencies. Operation outside this range automatically degrades antenna performance due to inherent mismatch between the antenna and the feed.

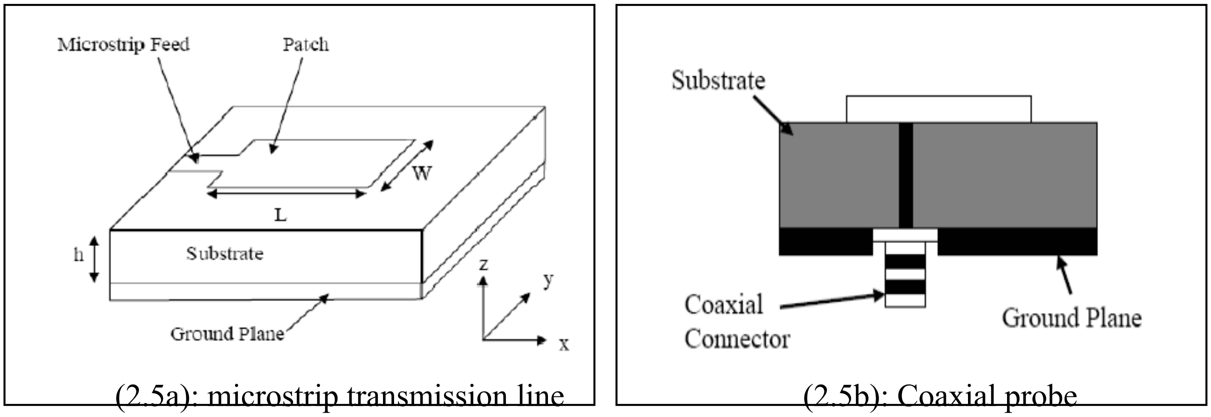

(2.5a): microstrip transmission line

(2.5b): Coaxial probe

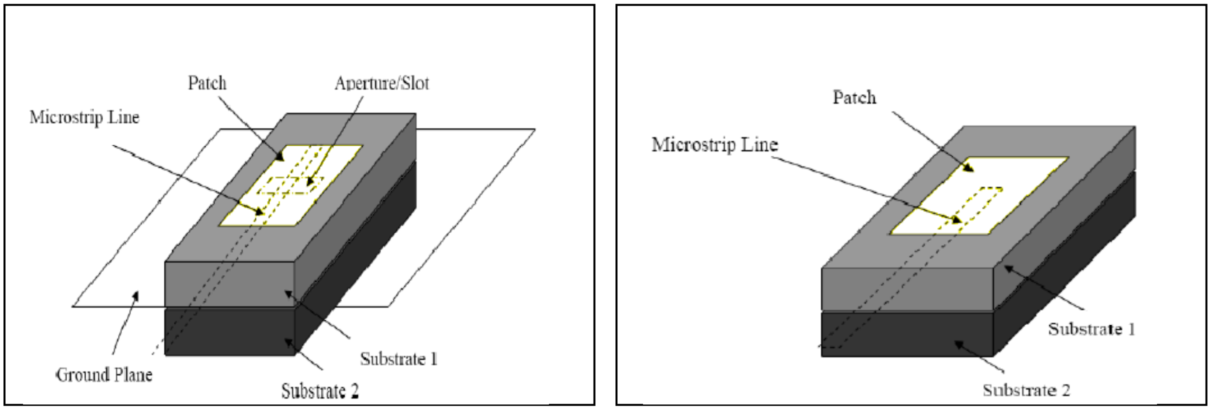

(2.5c): aperture coupling

(2.5c): Proximity coupling

Figure 2.5: Feeding Methods

2.5 Methods of analysis

In common practice, microstrip antennas are evaluated using one of the three analysis methods – the transmission line model, the cavity model, or the full wave model (which include primarily integral equations/Moment Method). [1]

The transmission line model is the easiest of all, it gives good physical insight, but is less accurate and it is more difficult to model coupling. Compared to the transmission line model, the cavity model is more accurate but at the same time more complex. However, it also gives good physical insight and is rather difficult to model coupling, although it has been used successfully. In general when applied properly, the full wave models are very accurate, very versatile and can treat single elements, finite and infinite arrays, stacked elements, arbitrary shaped elements and coupling. However, they are the most complex models and usually give less physical insight.

2.6 Summary

In this chapter, microstrip antenna was introduced together with its basic structure. The advantages and disadvantages are also being described. The basic properties of microstrip antenna are well defined in this section. This chapter focusing on the feeding methods and the methods of analysis that will be vital in this project later on.

CHAPTER 3

ELECTROMAGNETIC BAND GAP (EBG)

3.1 Introduction

The birth of the electromagnetic band gap structure has triggered many novel antennas applications. Two commonly employed features are suppressing unwanted substrate modes and acting as an artificial magnetic ground plane. Today, many antennas are required to be small and broadband. Conventionally, in order to achieve small size and broadband operation patch antenna are fabricated on a thick piece of high permittivity substrate. There are two major disadvantages in this, firstly, the higher the relative permittivity of a material the more costly it would be. Second, unwanted substrate modes begin to form and propagate towards the edges of the substrate, which have a deleterious effect on the antenna radiation pattern. One can expect an increase in back radiation level, distortion of the main lobe and side lobes appearing.[14]

In the 1990s, researches suggested the introduction of an electromagnetic band gap structure into the printed antenna substrate, which saw the capability of removing unwanted substrate modes. This EBG substrate has two commonly employed configurations namely the perforated and metallodielectric structures. The former consists of the periodic arrangement of air-columns. The effectiveness of the perforated structure relies on the high refractive index contrast between the air-columns and the relative permittivity of the dielectric material and the type of the lattice to use. For broadband and small volume mobile communication applications, the honeycomb-lattice was shown to be of good potential.

However, unless the substrate has a high relative permittivity, it is more appropriate to employ the metallodielectric structures simply because they are usually easier to manufacture and have wide range of applications. They consist of periodic metalized elements etched usually on the same layer as the microstrip antenna with metal vias connecting the periodic patches on the ground. In most cases, vias are necessary to prevent waves with non-zero vertical electric field component to travel between patch array and the ground.[16]

3.2 Formation of surface wave (surface plasmon)

As a patch antenna radiates, a portion of the total available power for direct radiation becomes trapped along the surfaces of the substrate. This trapped electromagnetic energy leads to the development of surface waves. [4] In fact, the ratio of power that radiates into the substrate compared to the power that radiates into air is approximately $(\varepsilon^{3/2}:1)^{5}$. This is governed by the rules of total internal reflection, which state that any field line radiated into the substrate at angles greater than the critical angle $(\theta_c = \sin^{-1}(\varepsilon^{-1/2}))$ are totally internally reflected at the top and bottom surfaces. This is illustrated in Figure 3.1. Therefore, for a substrate with dielectric constant $\varepsilon = 10.2$, nearly 1/3 of the total radiated power is trapped in the substrate with critical angle of roughly 18.2 degrees.[18]

Surface wave effects can be eliminated by using cavities or stacked substrate techniques. However, this has the fundamental drawback of increasing the weight, thickness, and complexity of the microstrip antenna, thus negating many of the advantages of using microstrip antennas. These complications and others prevent microstrip antennas from becoming the standard in the microwave telecommunications community.

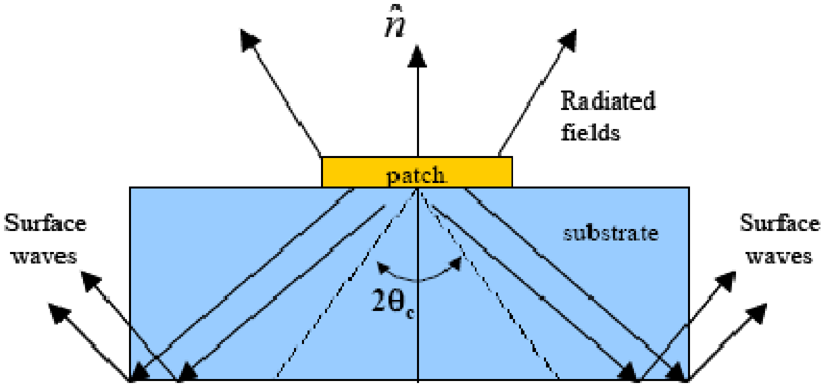

Figure 3.1: Field lines radiating from a patch antenna; illustrates the formation of surface waves

3.3 Perforated EBG structure

The first electromagnetic band gap (EBG) structure (previously termed Photonic band gap (PBG)) conceptualized and manufactured was in 1991 by Eli Yablonovitch, then at Bell Communications Research in New Jersey. Yablonovitch fabricated the crystal structure by mechanically drilling holes a millimeter in diameter into a high dielectric constant material (perforated EBG structure) as shown in Figure 3.2. This patterned material, which became known as “Yablonovitch” prevented incident microwave signals from propagating in any direction along a unit sphere – in other words, it exhibited a 3-D band gap.[5][6] This structure has become the cornerstone for much of the researcher in this area with applications still in use today. [7]

In most communication applications, however, the use of Yablonovitch is not practical. The three dimensional nature of the band gap rejects incident energy from all directions around a unit sphere, making it better suited as a high efficiency reflector or mirror. Instead, in a 2-D photonic crystal, the band gap exists only within a plane, thereby allowing propagation along one axis of the crystal. This is the ideal scenario for microstrip antenna designs, since the “rejection plane” could be in the plane of the patch to prevent surface wave’s formation. An example of a 2-D photonic crystal is a triangular lattice, as shown in Figure 3.3.

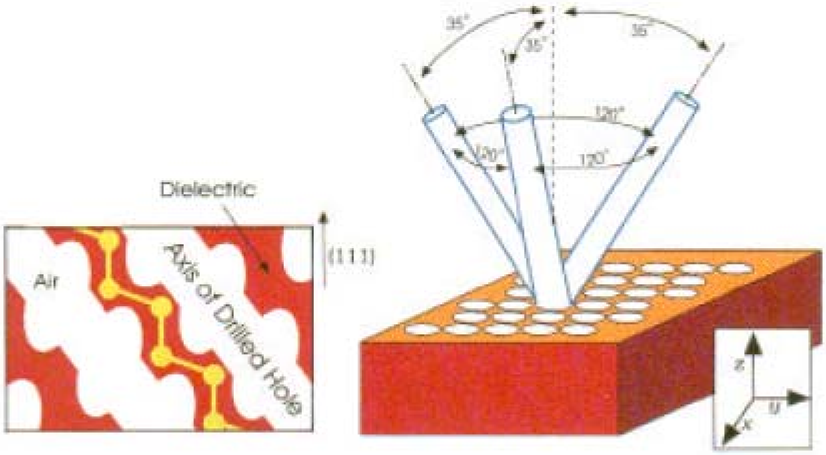

Figure 3.2: Technique used to fabricate the first 3D PC structure, the Yablonovite

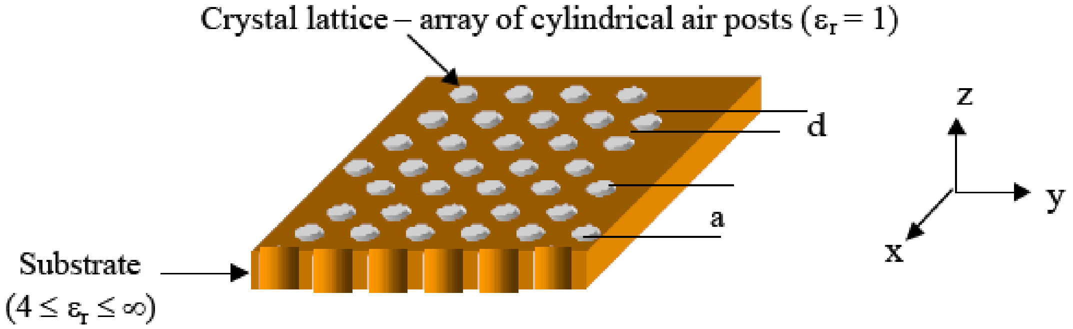
Crystal lattice – array of cylindrical air posts ($\varepsilon_r = 1$)
d
a
Substrate
($4 \leq \varepsilon_r \leq \infty$)
z
y
x

Figure 3.3: 2D photonic crystal structure patterned with a triangular crystal lattice; the crystal lattice is of cylindrical air posts in a high dielectric substrate.

A photonic crystal essential behaves much like a band-stop filter, rejecting the propagation of energy over a fixed band of frequencies. However, once a defect is introduced such that it disrupts the periodicity in the crystal, an area to localize or “trap” electromagnetic energy is established. In this region, a pass-band response is created. This ability to confine and guide electromagnetic energy has several practical applications at microwave frequencies as filters, couplers, and especially antennas.

This rather simple concept of placing defects in a photonic crystal structure introduces a new methodology in the design of microstrip (patch) antennas. The idea is to design a patch antenna on a 2D photonic crystal substrate, where the patch becomes the "defect" in the crystal structure, as shown in Figure 3.4. In this case, crystal arrays of cylindrical air holes are patterned into the dielectric substrate of the patch antenna. By not patterning the area under the patch, a defect is established in the photonic crystal, localizing the EM fields. Surface waves along the XY plane of the patch (Figure 3.4) are forbidden from forming due to the periodicity of the photonic crystal in that plane. This prevention of surface waves improves operational bandwidth and directivity, all while reducing side lobes and coupling, which commonly concerns in microstrip antenna designs.

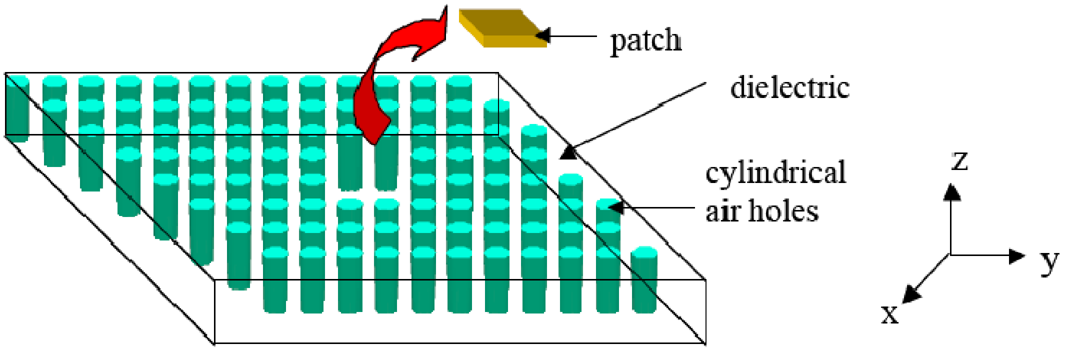

Figure 3.4: Illustration of a patch designed on a photonic crystal substrate; defect introduced in the area under the patch

Although "photonic" refers to light, the principle of "band gap" applies to electromagnetic waves of all wavelengths. Consequently, there is a controversy in the microwave community about the use of the term “Photonic”, and the name Electromagnetic band gap (EBG) material or Electromagnetic crystal is being proposed.

3.4 Metallodielectric EBG structure

The Metallodielectric EBG structure can act as an engineerable, artificial metal. These structures completely expel electromagnetic wave just as metals do. Like metals, they also support surface currents. By engineering the geometry of the surface, it can produce a structure that also has a band gap for the surface currents which overlaps the bulk band gap. This new materials should be useful as a ground plane in low profile antenna application (in this case: microstrip antenna).

Metallodielectric Electromagnetic Band Gap (MEBG) arrays have been placed over a ground plane in order to significantly enhance the directivity of simple radiating sources positioned between the array and the ground [8][9]. The structure is based on the formation of a resonant cavity between the ground plane and the array that acts as a partially reflective surface (PRS). The significant gain enhancement of microstrip patches and grounded waveguide apertures has been demonstrated. Similar implementations using dielectric EBG superstrates have also been presented and novel explanations have been given. [10][11]

3.5 Applications of electromagnetic band gap (EBG) structure.

Today metallodielectric electromagnetic band gap structures are well understood by the microwave community. Other properties of such structures are still being very actively investigated. In this section, there are two applications of EBG structure being discussed.

3.5.1 A multi-period EBG structure for microstrip antenna

In this paper, the author proposed to build a microstrip patch antenna on a 2-D multiperiod EBG structure. The EBG layer is sandwiched between the patch and the ground plane, as shown in Figure 3.5. The patch antennas on the proposed multiperiod EBG structure and a single period EBG structure were evaluated using the CST Microwave Studio package, which based on a Finite Integral technique being equivalent to FTDT in the time domain. The modeled antennas are then fabricated and measured at QMUL (Queen Mary, University of London) Antenna Lab.

The conventional patch antenna, which is designed for comparison with the proposed patch antenna on the sandwiched multiperiod EBG, is shown in Figure 3.5(a). The dimensions of the antenna is 8.3mm(W) x 6mm(L) and the substrate size is 78mm(W) x 63mm(L) with dielectric constant of 10.2, thickness 2.5mm(RT/Duroid 6010). A 50Ω microstrip line with width of 0.6mm is used here to feed the microstrip antenna up to the 50Ω feed point. A resonant frequency of 7.4GHz is obtained with these parameters.

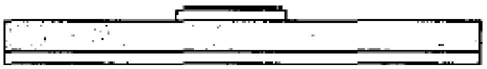

(a) Conventional patch antenna

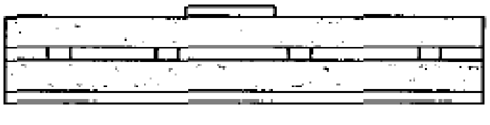

(b) Patch antenna on the sandwiched EBG structure

Figure 3.5: Cross section views of the patches of the conventional and sandwiched EBG substrates

The period value of a= 12mm is used for the single period EBG structure. For the multiperiod EBG structure, the period around the centre of the substrate remains as 12mm while the period around the edge of the substrate is reduced to 7.5mm. The 8 x 6 circles with radius of 3mm are etched on the sandwiched EBG layer for both single and multiperiod EBG structure as shown in Figure 3.6(a) and 3.6(b). It was noticed that the patch antenna does not overlap with any unit circle a better performance can be obtained. It can be seen that the size of the multiperiod EBG structure is substantially reduced.

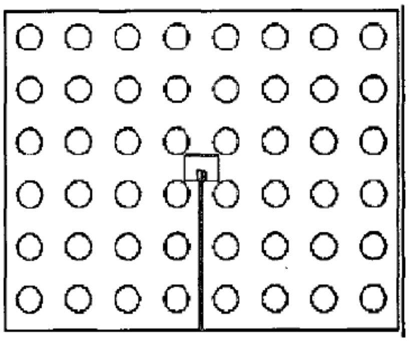

(a) Single period, a,=12mm EBG structure. Ground plane dimensions = 96mm(W)x 72mm(L)

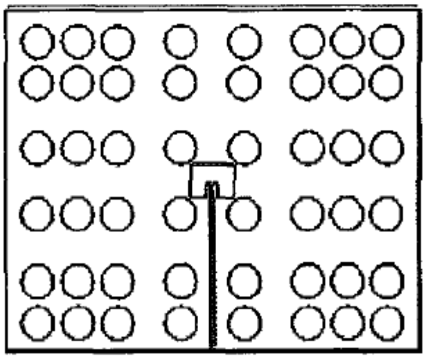

(b) Multiperiod,a_1= 12mm and a_2= 7.5mmEBG structure. Ground plane dimensions = 78mm(w) x 63mm(L).

Figure 3.6: Schematic of the single and multi period EBG structure sandwiched between the patch antenna and ground plane.

The input return loss (S11) for these three antennas obtained from simulations and measurements are shown in Figure 3.7(a), 3.7(b) and 3.7(c) respectively. Figure 3.7

shows that from the simulations the S11<-10dB bandwidth increases from 1.08% for conventional antenna to 1.36% for the antenna on the multiperiod EBG structure while it only increases to 1.25% for the antenna on the single period EBG structure. The measured results also show the increases of impedance bandwidth for the antenna on the multiperiod EBG structure. The multiperiod EBG design not only provides wider bandwidth over the other two designs but it also requires a small dimension of ground plane when compared with single period EBG structure. Besides that, the antenna on the multiperiod EBG structure has the lowest return loss, S11 at the resonant frequency compared to the other two antennas in both simulated and measured results. It is noticed that the difference between the simulated and measured resonant frequencies is slight bigger for the antennas on the sandwiched EBG structure than that for the conventional patch antenna. This might be due to the imperfection in manufacturing the sandwiched EBG substrate.

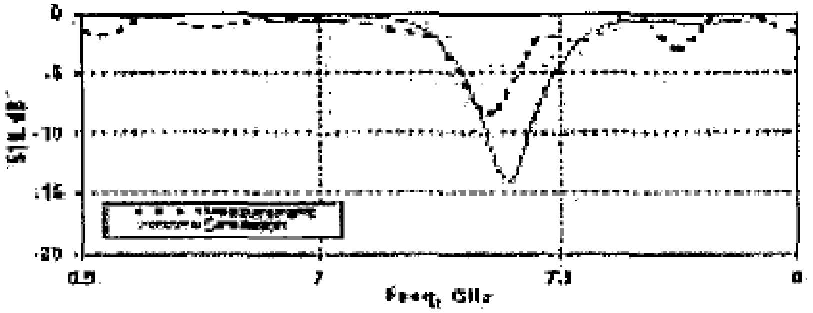

(a) Conventional patch antenna

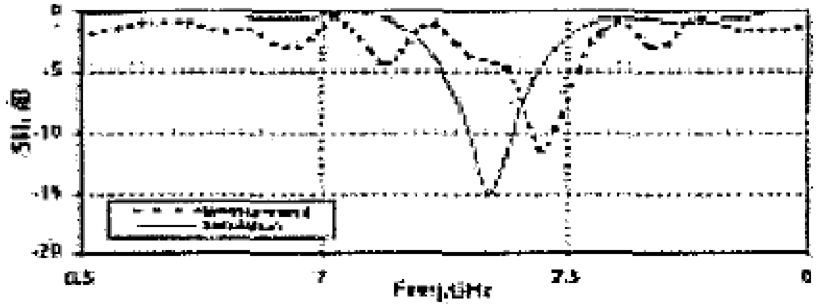

(b) Single period, a= 12mm EBG antenna

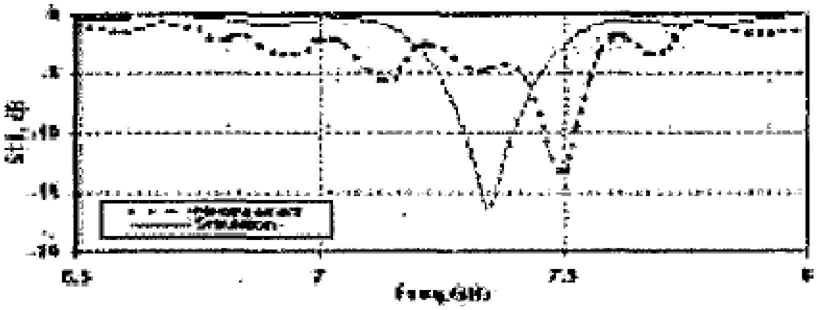

(c) Multiperiod a_1 = 12mm and a_2= 7.5mm, EBG antenna

Figure 3.7: Simulated (solid line) and measured (dotted line) input beam loss (S11) for conventional and two antennas on the sandwiched EBG structure.

Figure 3.8 shows the simulated and measured H-and E- plane radiation patterns of the three patch antennas. It can be observed from the H-plane radiation pattern of the antenna on the sandwiched multiperiod EBG substrate that the beam is narrower, compared to the other two antennas. This indicates effective surface wave suppression.

It is noticed in Figure 3.8 that the E-plane cuts for three antennas are asymmetry and broader compared with the H-plane cuts. There are also two peaks in E-plane cuts due to the radiation from the feed line. The gain in the forward direction for the conventional patch, the two patches on the single period and multiperiod EBG structures are 2.15dB, 3.55dB and 4.21dB respectively. This shows that there is a 2.06db of gain improvement on the multiperiod EBG substrate compared to the conventional substrate.

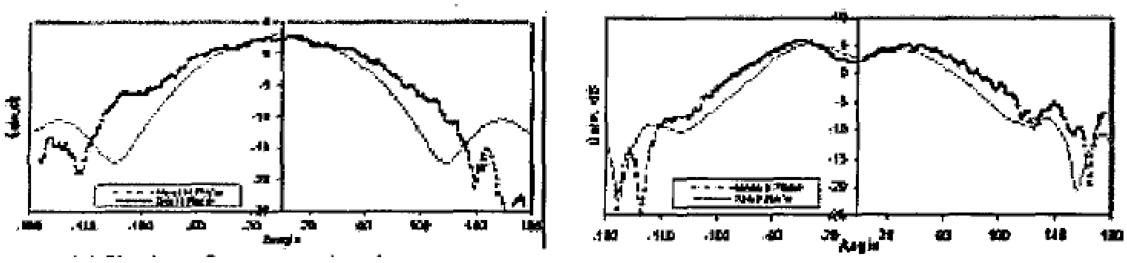

(a) H-Plane and E-Plane for conventional antenna

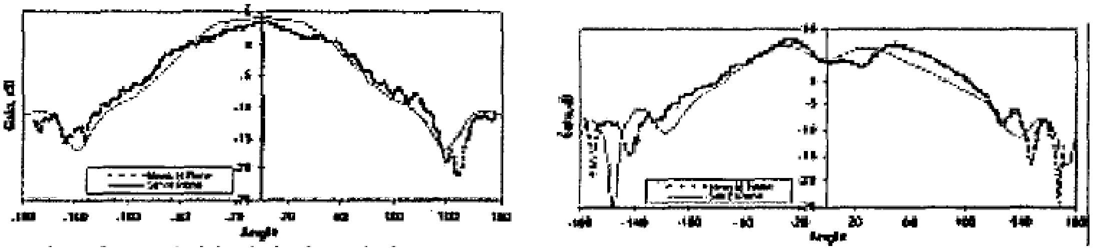

(b) H-Plane and E-Plane for sandwiched single period EBG antenna

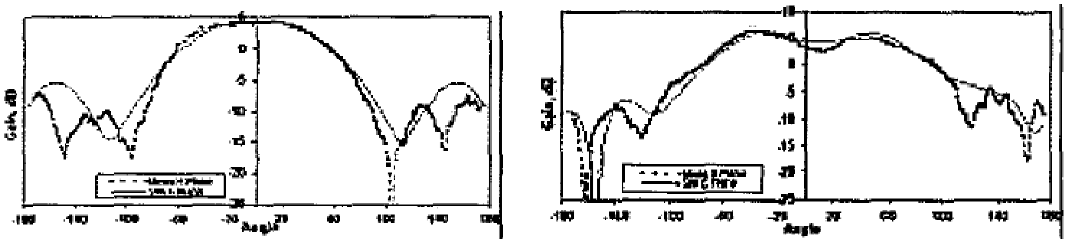

(c) H-Plane and E-Plane for sandwiched multiperiod EBG antenna

Figure 3.8: Simulated (solid line) and measured (dotted line) radiation patterns for conventional patch and two patches on the single period and multiperiod EBG structure.

As a conclusion, this paper has shown that the proposed embedded multiperiod EBG structure has advantages over the conventional and single period EBG substrate. With a 2-D multiperiod EBG structure, wider bandwidth is obtained and surface waves are suppressed as shown from the simulation and measurement results. Reduction in the surface waves will give a reduction in mutual coupling for antenna array applications.

3.5.2 Wideband microstrip patch antenna with EBG substrate

Single layer of EBG substrates were helpful for improving the gain of microstrip patch antennas, but had no effects on improving the bandwidth.[] For microstrip patch antennas over a single layer EBG substrates, the bandwidth achieved was narrow (<5%). Electrically thick substrates, with low dielectric constants, can increase the bandwidth. Thus, in this paper, the author placed another dielectric layer above the original EBG dielectric, to form a two layer EBG substrate. The geometry of this configuration is shown in Figure 3.9. In this structure, the metal patches used are 8mm by 8mm; the spacing between them is 0.2mm. For the substrate, the relative dielectric constant $\varepsilon_r = 2.5$, and the height $h_1=h_2=1.59$mm.

In order to find the bandgaps of the two layer EBG structure in Figure 3.9, Ansoft Ensemble was used to measure the radar cross section (RCS) vs. frequency, due to a plane wave incident horizontally on the structure. The result is shown in Figure 3.10. It can be seen that, the RCS has two peak reflections between 4.41 to 5.38GHz and between 8.31 to 11.72GHz. In this paper, the author presents the antenna properties with EBG substrates within the second bandgap (8.31-11.72GHz), because this range has much higher RCS magnitude than the first one.

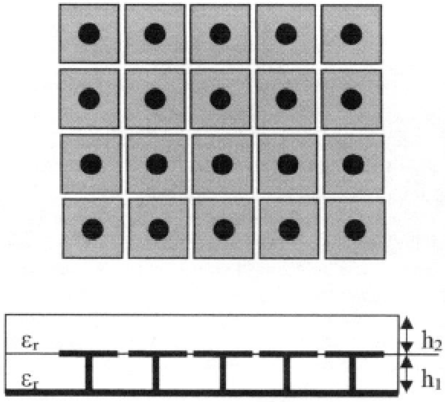

Figure 3.9: Geometry of a two layer EBG structure

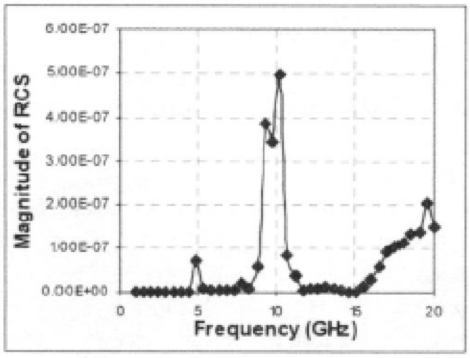

Figure 3.10: Magnitude of RCS vs. frequency on a two layer EBG structure with $\varepsilon_r = 2.5$, $h_1=h_2=1.59$mm, wave incident horizontally with vertical polarization.

The reference antenna was designed to work at 9.9GHz, and its parameters are listed as follows: Antenna length, L= 9mm, width, W= 4mm, dielectric constant $\varepsilon_r = 2.5$, substrate height, h= 1.59mm and the feed location L_f= 0.8mm. The ground plane was finite and had dimension of 60mm by 60mm. The achieved -10dB impedance bandwidth is narrow, which is 3.85% (9.67-10.05GHz). The simulated radiation patterns in the E and H plane are shown in Figure 3.11(a) and (b). As seen from the gain plots, the E plane co-polar pattern is wider than the H-plane co-polar pattern, and has a dip at $\theta = 0°$, which is caused by the size of the ground plane. The gain is 4.66dBi at $\theta = 0°$, and the peak gain is 6.03dBi. The H plane cross-polarization has a peak level of -6.10dBi, while the E plane cross-polar pattern is negligible and is not visible in this plot, because its value is lower than -30dBi. There is a large amount of back radiation caused by the diffraction from the ground planes edges and its value reaches -7.5dBi at $\theta = 95°$ and -11dBi at $\theta = 180°$.

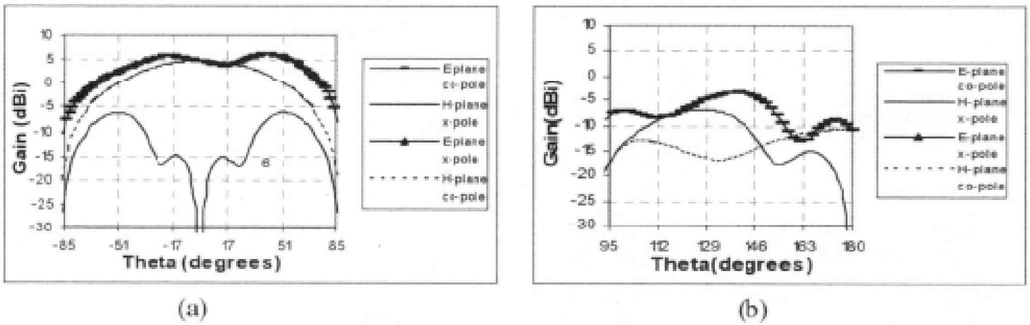

Figure 3.11: Radiation patterns of the reference antenna with L=9mm, W= 4mm, ε_r = 2.5, h=1.59mm, L_f= 0.8mm, ground plane: 60mm by 60mm (a) Front radiation (b) Back radiation

Next, the author designed an EBG antenna by placing grounding metal patches around the reference antenna. The dimensions of the EBG metal patches are 8mm by 8mm, the spacing between them is 0.2mm, and the vias used have a radius of 0.6mm. The bandwidth of the EBG antenna is still narrow, only 3.75% (9.69-10.06GHz), which is narrower than that of the reference antenna (3.85%). The E and H plane radiation patterns are shown in Figure 3.12, it can be seen that unlike the reference antenna, the E plane co-polar pattern is narrower than the H plane co-planar pattern, and the dip at θ = 0° of the E plane has disappeared. The gain of the EBG antenna is 8.98dBi at θ = 0°, which is 4.32dBi higher than that of the reference antenna. The peak level of the H plane cross-polarization has reduced to -10.76dBi, compared with -6.10dBi of the reference antenna. There is also a large amount of back radiation and its value is -5dBi at θ = 95° and -12.5dBi at θ = 180°.

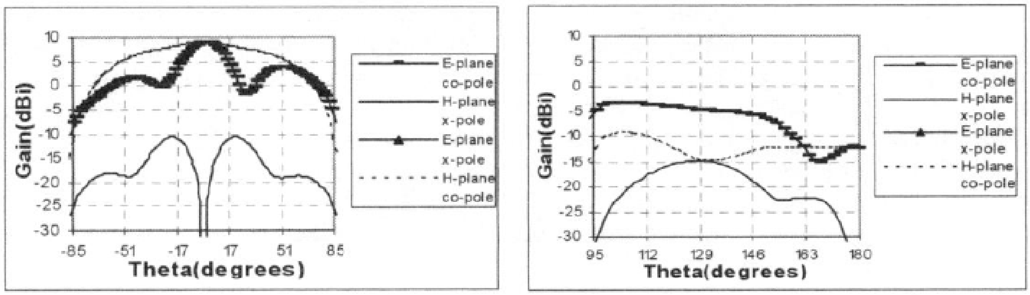

(a) (b)

Figure 3.12: E and H plane radiation patterns of a single layer EBG antenna with L=9mm, W= 4mm, ε_r = 2.5, h=1.59mm, L_f= 0.8mm, ground plane: 60mm by 60mm at 9.87GHz (a) Front radiation (b) Back radiation

In order to study the antenna properties with EBG substrates within the second bandgap, the author conducted the parametric study for the two layers EBG antenna, including the effect of feed location, antenna width, EBG position, X_0, Y_0 and the ground plane size. Finally, the optimized wideband EBG antenna was achieved and is shown in Figure 3.13. Its parameters are: L= 9mm, W= 4mm, ε_r = 2.5, h_1=h_2=1.59mm, L_f= 2.1mm, X_0= 12mm, Y_0=8.3mm. There are six EBG patches which have dimensions of 7.8mm by 8mm; the spacing between them is 0.1mm. The other EBG patches are 8mm by 8mm, and the spacing is 0.2mm. The ground plane is 60mm by 60mm. The simulated S_{11} for this antenna is shown in Figure 3.14. From the S_{11} plot, it can be seen that the -10dB impedance bandwidth reaches 24.69% (10.44-13.38GHz), which is a very wide bandwidth in the EBG field.

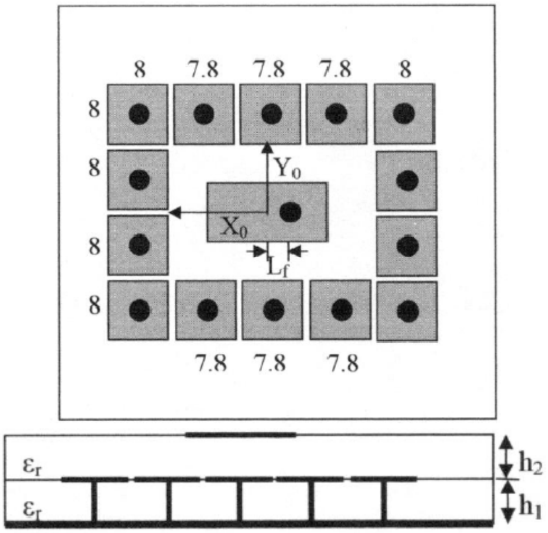

Figure 3.13:Geometry of the two layer EBG antenna with L=9mm, W =4mm, $\varepsilon_r = 2.5$, h1=h2=1.59mm, Lf =2.1mm, X0 =12mm, Y0 =8.3mm, EBG: 8mm by 8mm and 7.8mm by 8mm, spacing 0.2mm and 0.1mm, ground plane: 60mm by 60mm.

The radiation patterns for this optimized two layer EBG antenna at resonant frequency 11.36GHz are shown in Figure 3.15(a) and (b). From the gain plots, it can be seen that at resonant frequency 11.36GHz, the gain is 7.85dBi at $\theta = 0°$, which is 3.19dBi higher than that of the reference antenna (4.66dBi). But it is lower than that of the single layer EBG antenna (8.98dBi). The H plane cross-polarization has a peak level of -2.10dBi. The back radiation is -10dBi at $\theta = 95°$ and -11dBi at $\theta = 180°$.

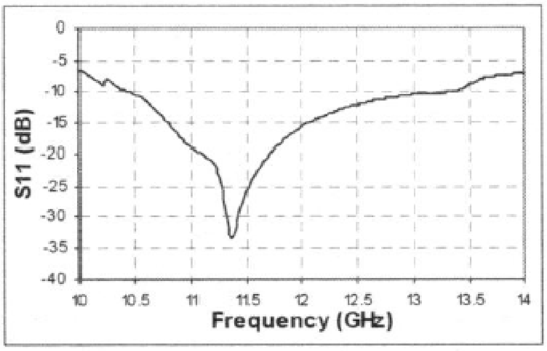

Figure 3.14: The S11 of the optimized two layer EBG antenna of Figure 3.13.

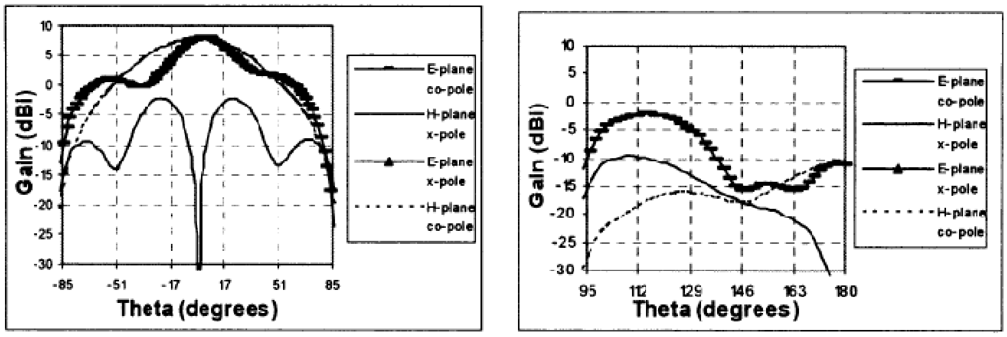

(a) (b)

Figure 3.15: E and H plane radiation patterns of the optimized two layer EBG antenna of Figure 3.13 at 11.36GHz (a) Front radiation (b) Back radiation.

As a conclusion, the two layers EBG structure was proposed in this paper. The bandgaps of the EBG structure were found by illuminating the structure with an incident plane wave and measuring the RCS vs frequency. By the parametric study for antennas with two layer EBG substrates, the wideband EBG antenna was achieved. The impedance bandwidth reached 24.96%, which is very wide in the EBG field. And the gain was more than 3dBi higher than that of the reference antenna.

3.6 Summary

Electromagnetic band gap (EBG) structure has been discussed in this chapter. The discussion covers from the formation of the surface waveform, the type of EBG structure and the publish applications. The two type of EBG structure are perforated and the metallodielectric EBG structure. The comparison between the two types will affect the fabrication process. So, the metallodielectric type has been selected to be further designed in this project due to ease of fabrication. Two applications being publish in antenna and microwave field also being discussed briefly.

CHAPTER 4

DESIGN METHODOLOGY

4.1 Conventional Microstrip antenna design

In order to identify and verify the improvement for electromagnetic band gap (EBG) structure in microstrip antenna, the conventional microstrip antenna was first designed.

4.1.1 Theoretical design

The first step in designing the patch antenna was to employ the following formulas as an outline for the design procedures.

i. Width (***W***):

$$W = \frac{c}{2fr\sqrt{\left(\frac{\varepsilon_r + 1}{2}\right)}}$$

where;

c - free space velocity of light, 3×10^8 m/s

fr - frequency of operation

ε_r - dielectric constant

ii. Effective dielectric constant (**ε_{reff}**):

$$\varepsilon_{reff} = \frac{\varepsilon_r + 1}{2} + \frac{\varepsilon_r - 1}{2}\left[1 + 12\frac{h}{W}\right]^{-1/2}$$

where;

ε_r - dielectric constant

h - height of dielectric substrate

W - width of the patch

iii. Effective length (**L_{eff}**):

$$L_{eff} = \frac{c}{2 fr \sqrt{\varepsilon_{reff}}}$$

where;

c - free space velocity of light, 3×10^8 m/s

fr - frequency of operation

ε_{reff} - effective dielectric constant

iv. Patch length extension (**ΔL**):

$$\Delta L = 0.412h \frac{(\varepsilon_{reff} + 0.3)\left(\frac{W}{h} + 0.264\right)}{(\varepsilon_{reff} - 0.258)\left(\frac{W}{h} + 0.8\right)}$$

v. Actual length of patch (**L**):

$$L = L_{eff} - 2\Delta L$$

4.1.2 Design Specifications

The antenna is designed to operate at frequency 2.4GHz. For this design, the FR4 dielectric material ($\varepsilon_r = 4.5$) with dielectric loss tangent (tanδ) of 0.019 and height of substrate (h) 1.6mm were used. The microstrip antenna is exited by a coaxial probe and the feed point is located at the distance (dx) away from the center of the patch.

The important parameters are summaries in the Table 4.1.

Table 4.1: Design parameters of microstrip antenna

Shape	Rectangular
Frequency	2.4GHz
Dielectric constant of substrate	4.5 (FR)
Height of substrate	1.66mm
Feeding method	Coaxial probe
VSWR	1.5:1
Gain	5dB – 8dB
Polarization	Linear

From the parameters describe above, the calculated value for length and width of the patch are L = 28.6 mm, W = 37.7 mm and the calculated position for the port is dx = 7.6mm from the edge of the patch.

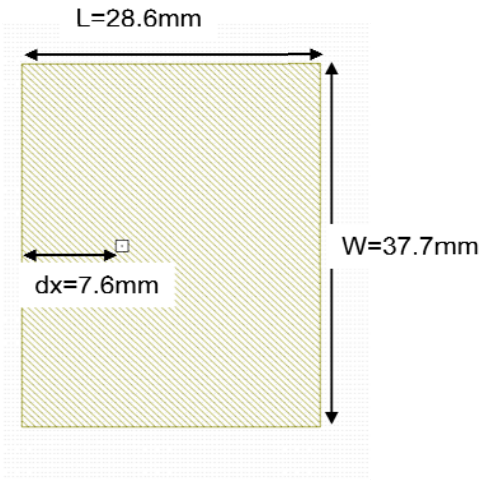

Figure 4.1: EM structure for conventional rectangular microstrip antenna

4.2 Electromagnetic band gap (EBG) structure design

The operation mechanism of EBG structure can be explained by an LC filter array. The central frequency of the band gap is $f_0 = 1/2\pi \; \overline{\quad}$. The inductor, L results from the current flowing through the vias, and the capacitor, C due to the gap effect between the adjacent patches. [10] The slot changes the current distribution on the patch. Additional capacitance is formed between the neighboring edges of the slot and the stretched strip from an adjacent patch. Increasing the depth of the stretched strip embedded in the slot, more capacitance will be introduced and vice versa. Thus variation of the depth of the stretched strip embedded in the slot results in the tuning of the frequency band gap position.

To the best of my knowledge, there are no exact formulas that relate the structural parameters of the EBG structure to the stop band frequencies. Therefore, the new EBG structure was designed using the parametric and experimental studies.

4.2.1 Design specification

The new EBG structure is designed to operate at frequency 2.4GHz. For this design, the FR4 dielectric material ($\varepsilon_r = 4.5$) with dielectric loss tangent ($\tan\delta$) of 0.019 and height of substrate (h) 1.6mm were used.

The whole EBG structure was selected with dimension of 34mm (width, W) x 35mm (length, L) with the single rectangular box of 10mm (width, W) x 7mm (length, L) and the vias with 1mm in diameter at the top left hand corner of the rectangular box structure.

The transmission line method is selected for analysis purposes. The stop band of an EBG structure needs to be generated directly using numerical simulation tool. The most direct method consists of extracting the scattering parameters (S-parameter) between two ports placed across the EBG structure.

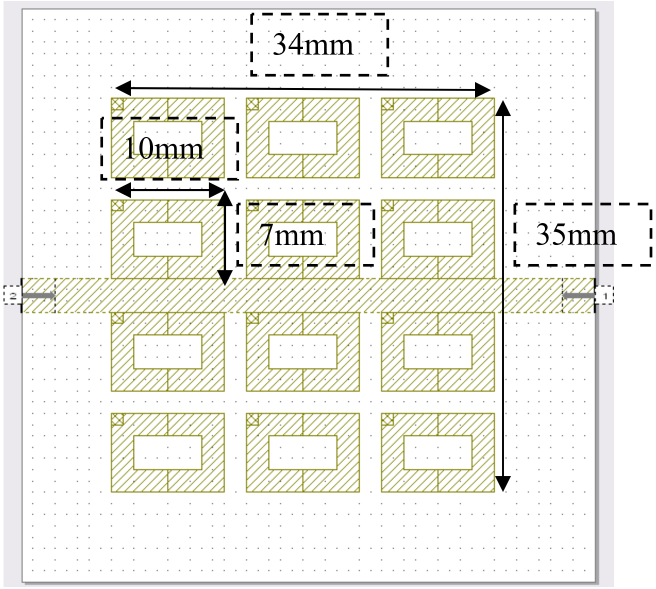

Figure 4.2: EM structure for EBG structure

4.3 Microstrip antenna with EBG structure

This design is basically the conventional microstrip antenna with the designed EBG structure placed on top and below of the structure (E- plane). The parameters are same as discussed in the conventional microstrip antenna and the EBG structure section.

4.4 Simulation

Microwave Office software was used to simulate the structure of the antennas. Microwave Office is a full-wave electromagnetic simulator based on the method of moments (MOM). Built on the unique AWR high-frequency platform with its open design environment and unified data model, Microwave Office design suite offers unparalleled ease-of-use, powerful technologies, and unprecedented openness and interoperability, enabling integration with best-in-class tools for each part of the design process. Microwave Office software includes all of the essential technology: linear and non-linear circuit simulators, EM analysis tools, integrated schematic and layout, statistical design capabilities, and parametric cell libraries with built-in DRC.

The software's intuitive graphical interface is used to design circuits composed of schematics and electromagnetic (EM) structures from an extensive electrical model database, and then generate layout representations of these design.

4.5 Fabrication

The fabrication process involves 5 steps as describe below:

4.5.1 Generate mask on transparency

First step is to transfer the EM structure from the Microwave Office software to Auto-Computer Added Drawing (AutoCAD) and print it onto the transparency film. Figure X shows the transparency film with the printed layout.

4.5.2 Photo exposure process

Second step is the Ultraviolet exposure process. It is done to transfer the image of the circuit pattern with a film in a UV exposure machine onto to the photo resist laminated board. The process took about 120 seconds (2 minutes).

4.5.3 Etching in developer solution

The third step is to ensure the pattern will be fully developed, during the developing process. The photo resist developer solution was used to wash away the exposed resist for about 10 minutes. Then the solution was removed by spray wash. In this process, water was added with Sodium Hydroxide (NaOH).

4.5.4 Etching in Ferric Chloride

Fourth step is the etching in ferric chloride. It will remove the unwanted copper area and this process was followed by the removal of the solution by water. This process took about 30 minutes to be done.

4.5.5 Soldering the probe

The final step was to solder the probe, where the board was dried and rubbed with sand paper to remove the remains of the unexposed resist pattern area. Upon fabrication, the SMA connector was soldered to the microstrip antenna.

The figures below show the 5 steps involve in the fabrication process.

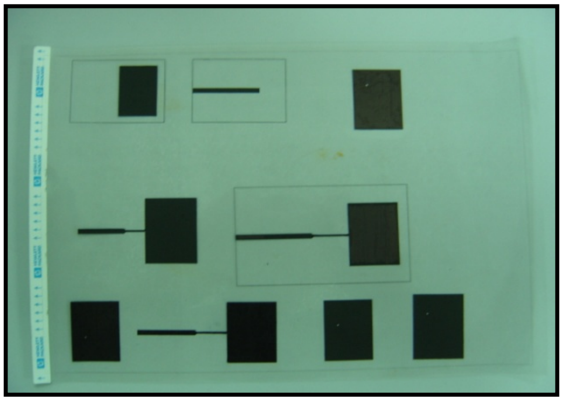

Figure 4.3: Circuit pattern on transparency

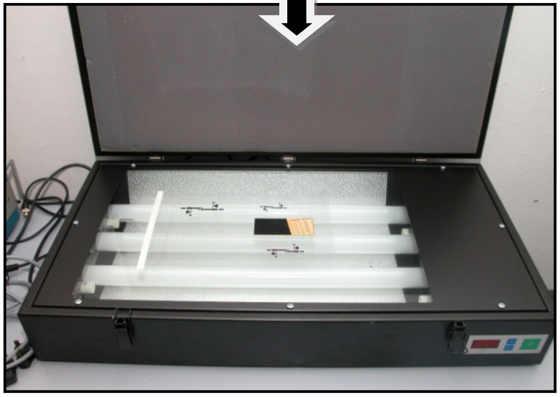

Figure 4.4: Photo exposure machine

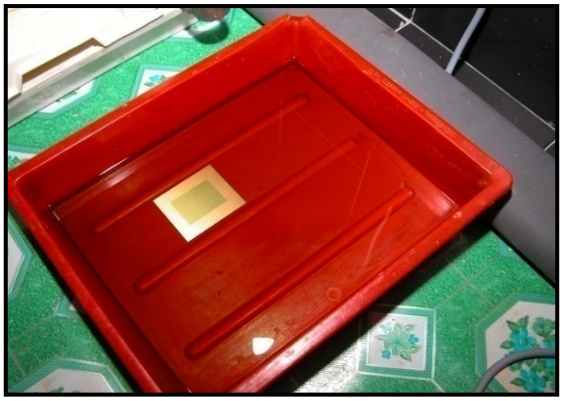

Figure 4.5: Etching in developer solution

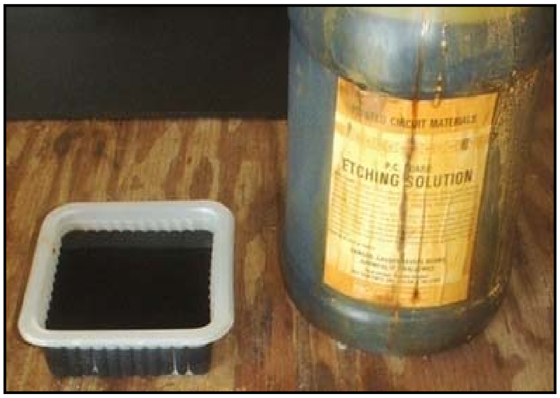

Figure 4.6: Etching in ferric chloride

e

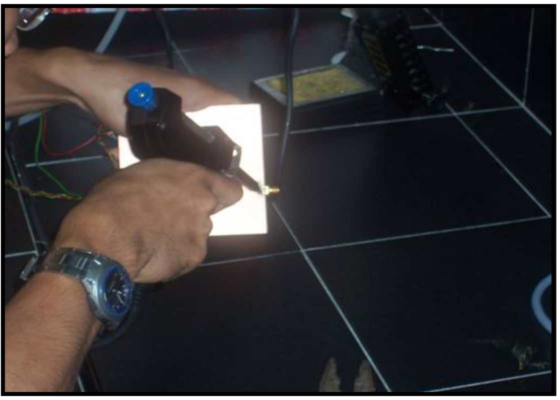

Figure 4.7: Soldering process

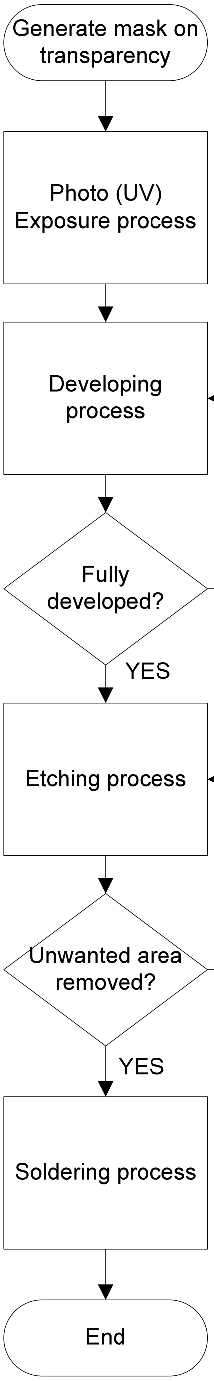

Figure 4.8: Flowchart of the fabrication process

4.6 Testing (Measurement)

The Microwave Test (network analyzer) set was used to measure the S11 and S21 of the antenna.

Figure 4.9: Marconi Scalar Analyzer 6204

4.7 Summary

This chapter explained the design methodology in designing the three structures that involve the conventional microstrip antenna design, the EBG structure design and the microstrip antenna with EBG structure design. The simulation and the fabrication process also being discuss in this section for references.

CHAPTER 5

SIMULATION AND MEASUREMENT RESULTS

5.1 Conventional Microstrip antenna

Based on the theoretical calculation describe in chapter 4, the conventional microstrip antenna was first designed as a reference. The dimensions of the conventional rectangular microstrip antenna are as shown in Figure 5.1 below. The rectangular patch, printed on a substrate of thickness, h and relative permittivity, ε_r, has a length, L and a width, W. The actual length of the patch is 28.6mm, the width of the patch is 37.7mm and a coaxial probe that excites the antenna is located at the distance (dx) of 7.66mm away from the edge of the patch. The 3D layout of the designed antenna with its coaxial feed line is as shown in Figure 5.3.

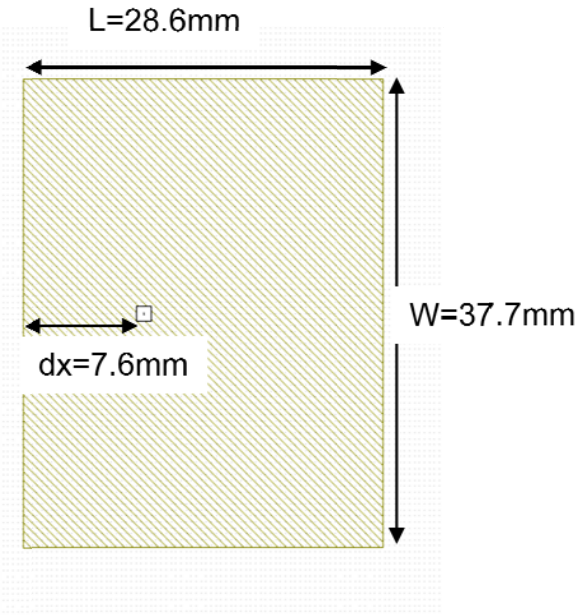

Figure 5.1: EM structure with the calculated value of W, L and port position.

The view of fabricated antenna for conventional rectangular patch is as shown in Figure 5.2 below.

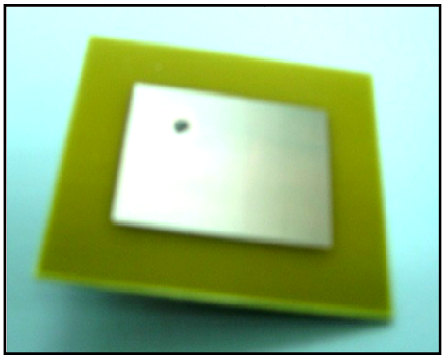

Figure 5.2: Fabricated structure of microstrip antenna

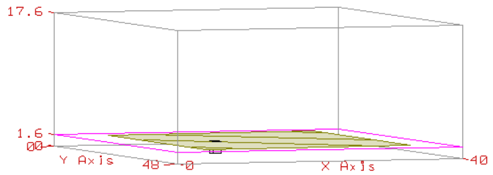

Figure 5.3: 3D layout of the conventional rectangular patch antenna with the coaxial feed.

Figure 5.4 shows the simulated result for return loss (RL) of the conventional patch antenna against frequency. As can be observed from the figure, the return loss for the conventional patch antenna is -20.68dB at 2.4GHz. A negative value of return loss shows that this antenna had not many losses while transmitting the signals.

From the same figure the antenna bandwidth was calculated by using this formula:

$$Bandwidth = \frac{f_2 - f_1}{\sqrt{f_2 \, x \, f_1}} x100\%$$

The value of f1 and f2 were taken at –10dB or 10% from the transmitted power.

$$Bandwidth = \frac{2.4266G - 2.3733G_1}{\sqrt{(2.4266Gx2.3733G)}} x100\% = 2.22\%.$$

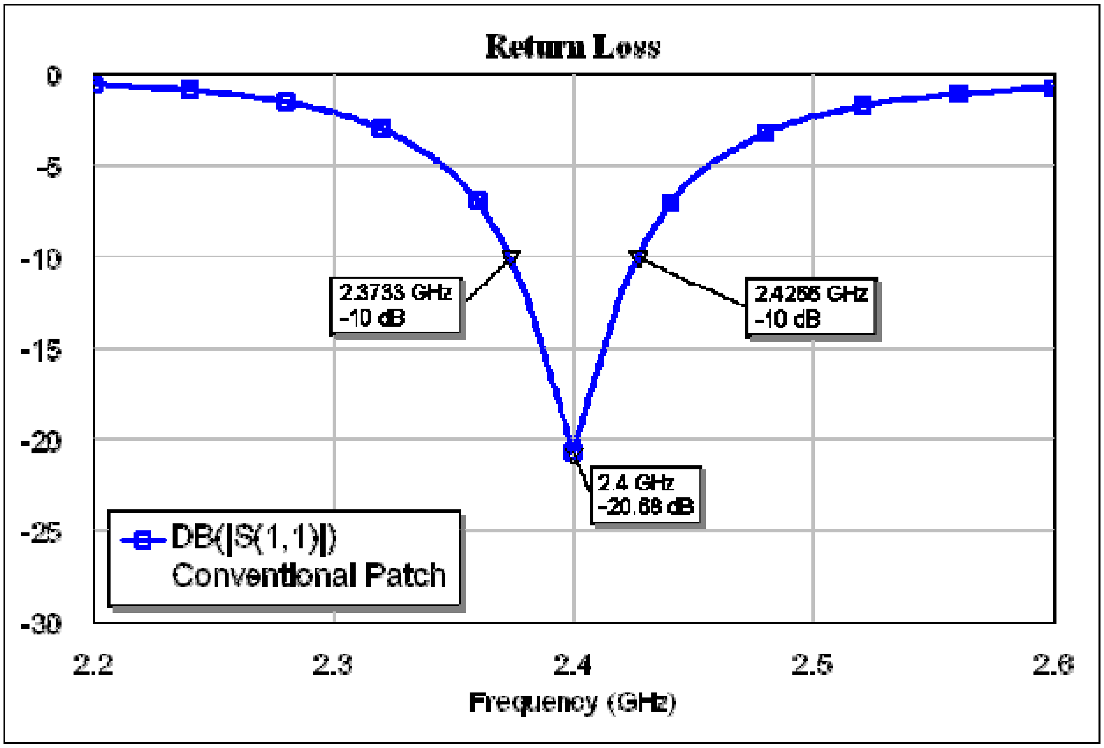

Figure 5.4: Return Loss for conventional rectangular patch antenna.

Since a microstrip patch antenna radiates normal to its patch surface, the elevation for Etheta = 0° and Ephi = 90° would be important. Figure 5.5 below shows the maximum radiation occurs at 0° with gain of 5.58dB.

This project aim is to improve the maximum radiation pattern for the microstrip antenna. Later on, the comparison of these parameters will be seen when the EBG structure was placed with the microstrip antenna.

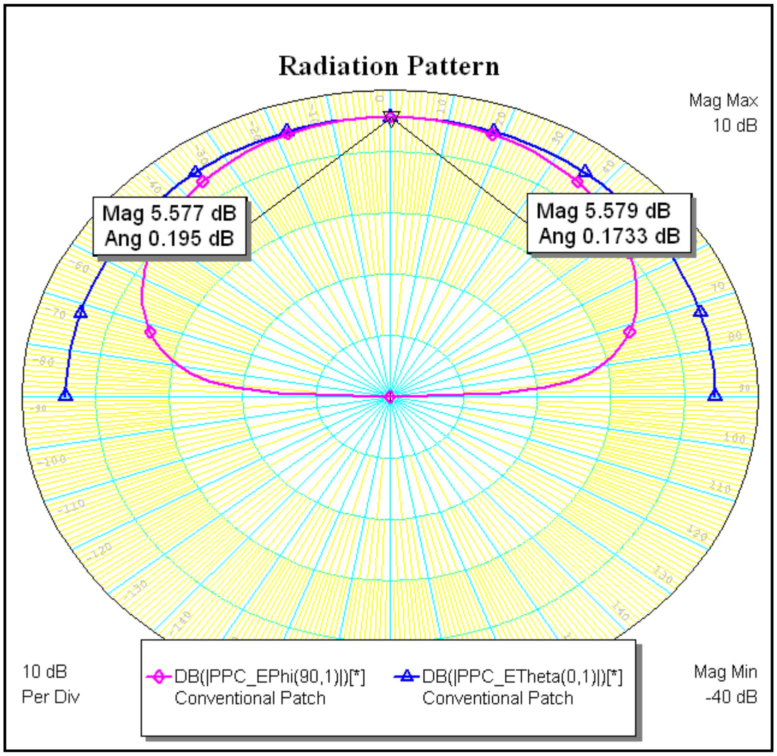

Figure 5.5: Maximum radiation at 0°, gain = 5.58dB for conventional rectangular patch antenna.

5.2 Electromagnetic band gap (EBG) structure

Critical parameters of an EBG structure are illustrated in Figure 5.6. These parameters include the size of individual patches, diameter of stubs (vias), thickness, and material of the substrate. The geometrical features of the structure and the substrate material directly relate to the frequency of the stop band.

The operating frequency is at 2.4GHz. In this design, the dimension of 34mm (width, W) x 35mm (length, L) with the single rectangular box of 10mm (width, W) x 7mm (length, L) and the vias with 1mm in diameter at the top left hand corner of the rectangular box structure was selected.

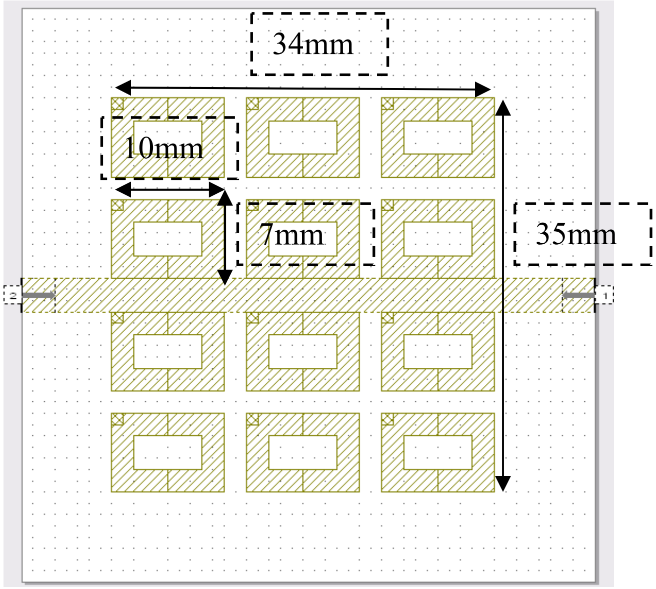

Figure 5.6: EM structure for the EBG.

The view of fabricated antenna for conventional rectangular patch is as shown in Figure 5.7 below,

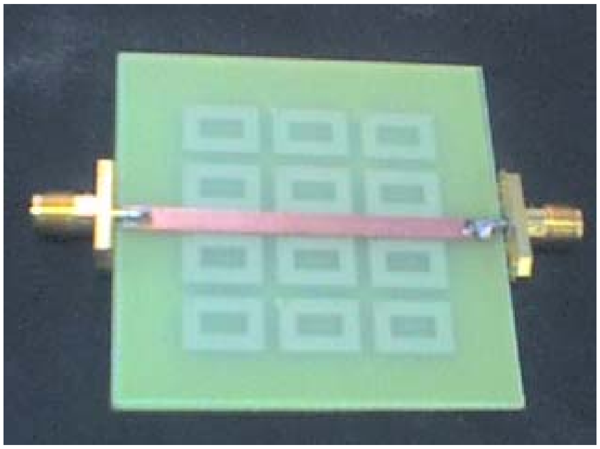

Figure 5.7: Fabricated view of EBG structure

The 3D layout of the designed antenna with its coaxial feed line is as shown in Figure 5.8.

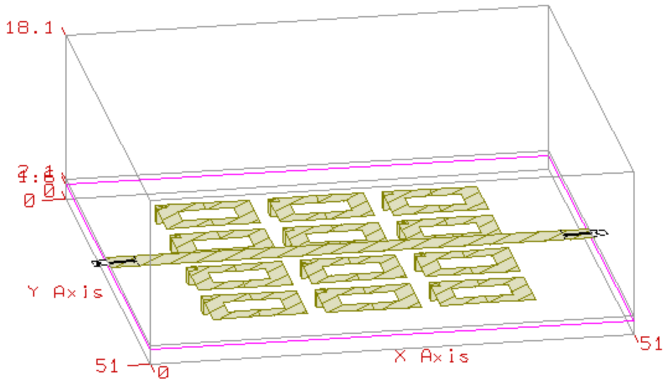

Figure 5.8: 3D layout of the EBG structure with the transmission line analysis method.

Figure 5.9 shows the simulation results of S21 parameter for the EBG structure. From this results, we can see that the EBG structure produce the stop band at 2.4GHz. The transmission from port 1 to port 2 was -34.94dB at 2.4GHz. This is the band gap characteristic of this structure.

From this simulation also, we can determine the structure bandwidth using the same formula for microstrip antenna. The value of f1 and f2 were taken at –20dB or 20% from the transmitted power and the bandwidth was computed to be 8.17%.

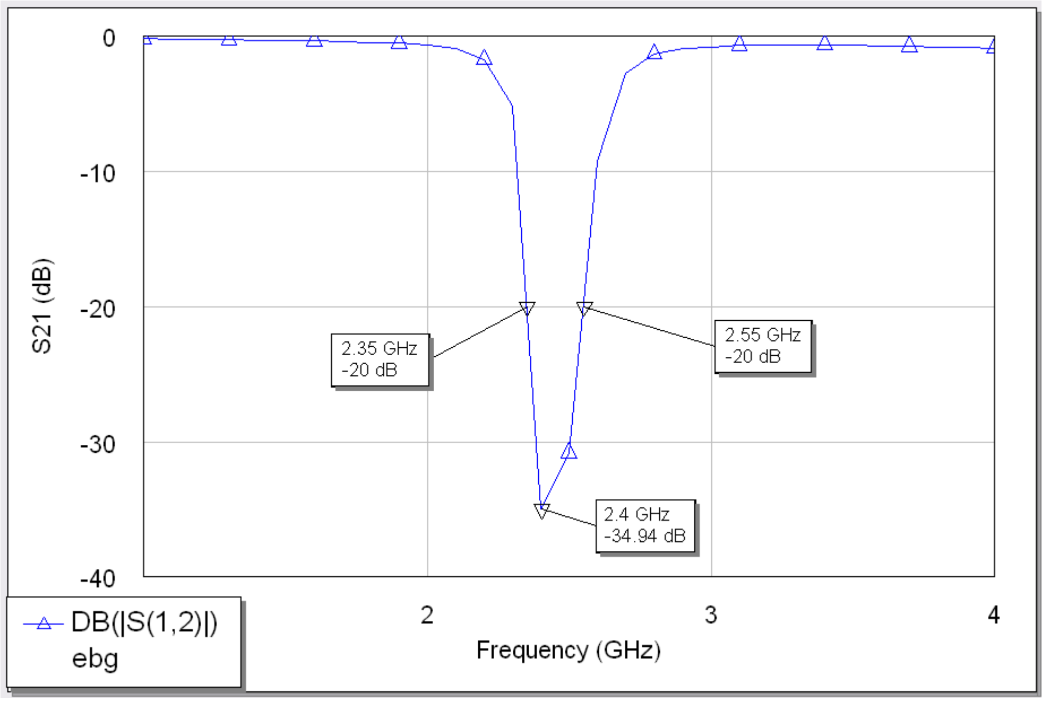

Figure 5.9: S21 parameter for the EBG structure.

The comparison for the simulated and measured EBG structure also being done and it show not much different in the value of S21.

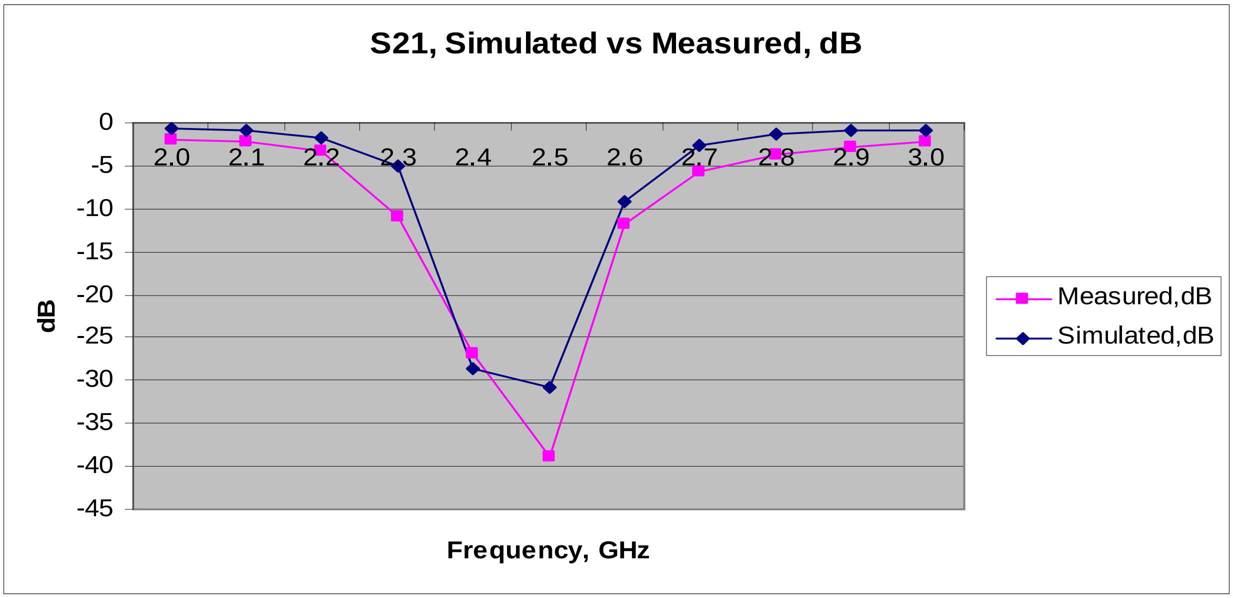

Figure 5.10: Comparison of S21 parameters between simulation and measurement values of the EBG structure.

5.2.1 Effect of the vias locations

The parametric study of the structure has been done for the appropriate vias locations and the separation (gap) of the single EBG structure as shown in Figure 5.11.

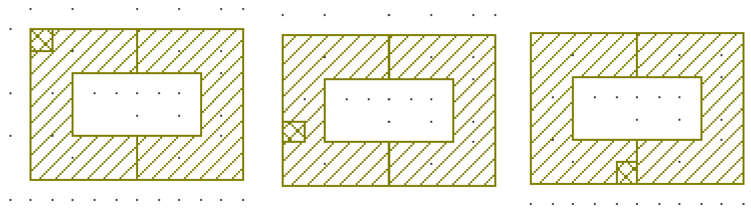

(5.11a) (5.11b) (5.11c)

Figure 5.11: Different location of the vias in the EBG structure.

Based on the simulated value, different position of vias lead to different value of frequency. For the first position (Figure 5.11a) the frequency is at 2.4GHz. As we move the via to 4mm (Figure 5.11b) below, the frequency shift to 2.697GHz, and the frequency shift to 2.8GHz when we move it to position as Figure 5.11c.

Based on this parametric study, we conclude that the best position of vias that operating at 2.4GHz frequency is in the Figure 5.11a and the frequency change as the position change.

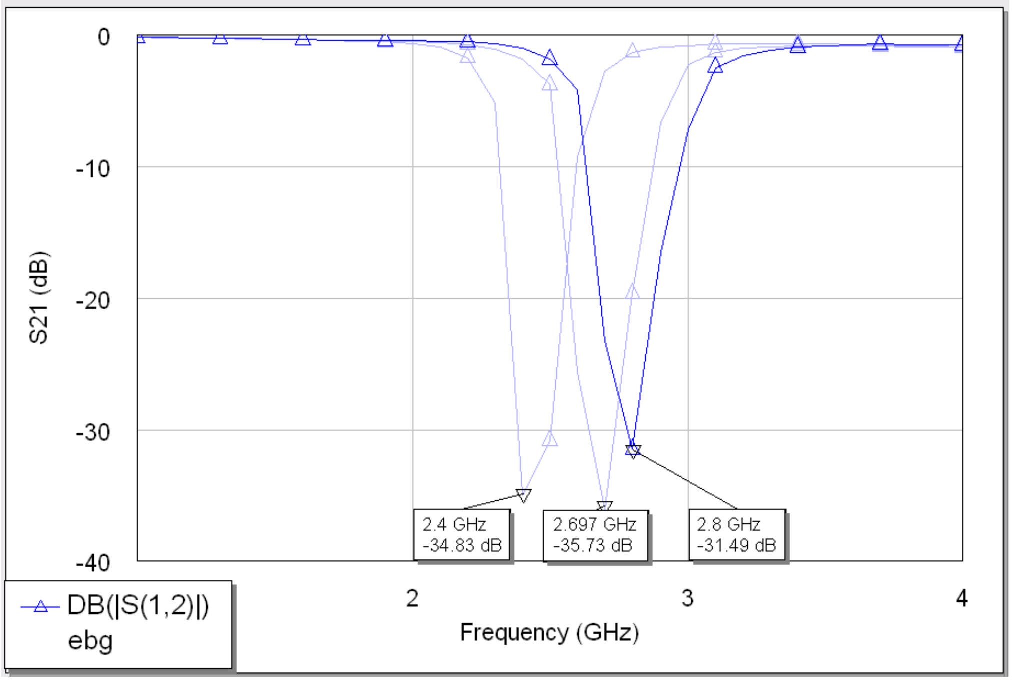

Figure 5.12: Comparison of S21 for the different location of vias.

5.2.2 Effect of the separation (gap) of the single EBG structure.

Another parametric study was done for the separation (gap) of the EBG structure. Three comparisons have been made for movement of 2mm and 4mm from the original structure.

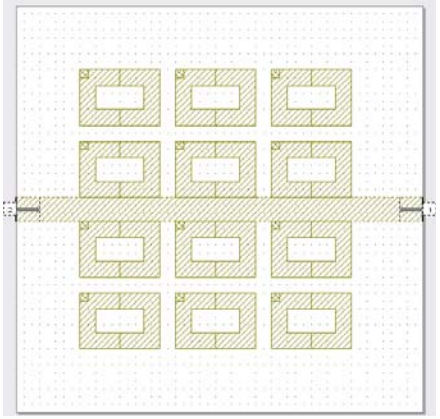

(5.13a)

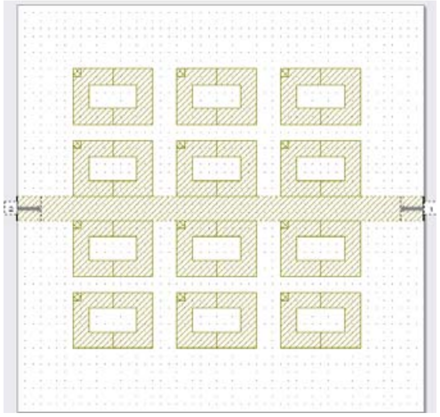

(5.13b)

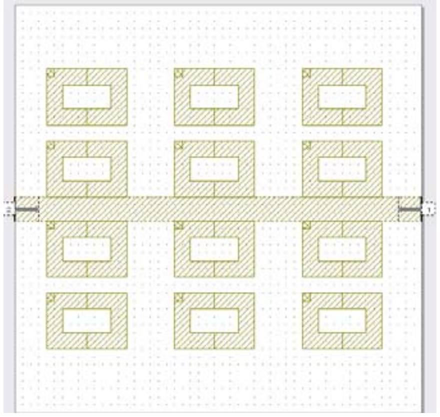

(5.13c)

Figure 5.13: Different separation (gap) of the EBG structure.

Based on the simulated values, we can see that different separation (gap) produce different gain in S21 parameters. The operation frequency has no effect for this study. For the original structure (Figure 5.13a), the transmission coefficient was simulated at -34.94dB. As we can see, the transmission coefficient in S21 parameter increases as the gap increases. For structure as Figure 5.13b the transmission coefficient is -37.28dB and the transmission coefficient is -52.03dB for structure in Figure 5.13c.

We can conclude that, the further the separation, the transmission coefficient of S21 parameter increases. But for the ease of fabrication and to reduce size, the first (Figure 5.13a) was selected as the new design EBG structure.

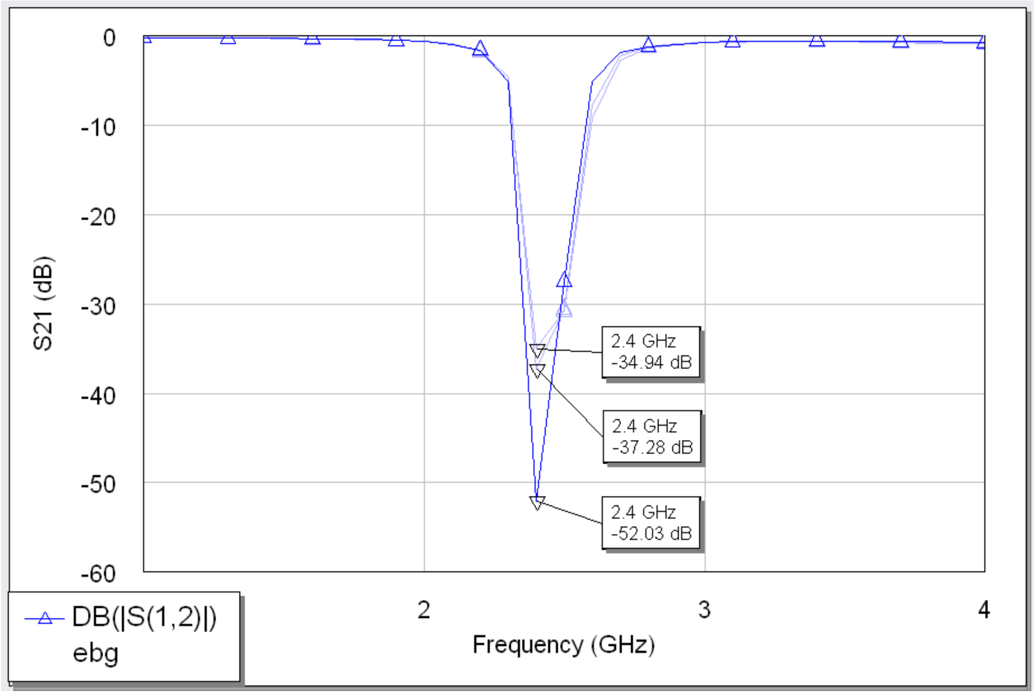

Figure 5.14: Comparison of S21 parameters for different separation gap of EBG structure.

5.3 Microstrip antenna with EBG structure

This design basically to verify the improvement of the radiation pattern of microstrip antenna when we introduced the EBG structure with it. The parameters involve are the same for the dimension of conventional microstrip antenna as well as the EBG structure.

The overall dimension for this structure is 34mm (Width, W) x 53mm (Length, L). It is shown that the EBG structure only being placed on top and bottom of the microstrip antenna (E- plane). This is because the H-plane have much smaller mutual coupling than E-plane couples ones between the elements next to each other.

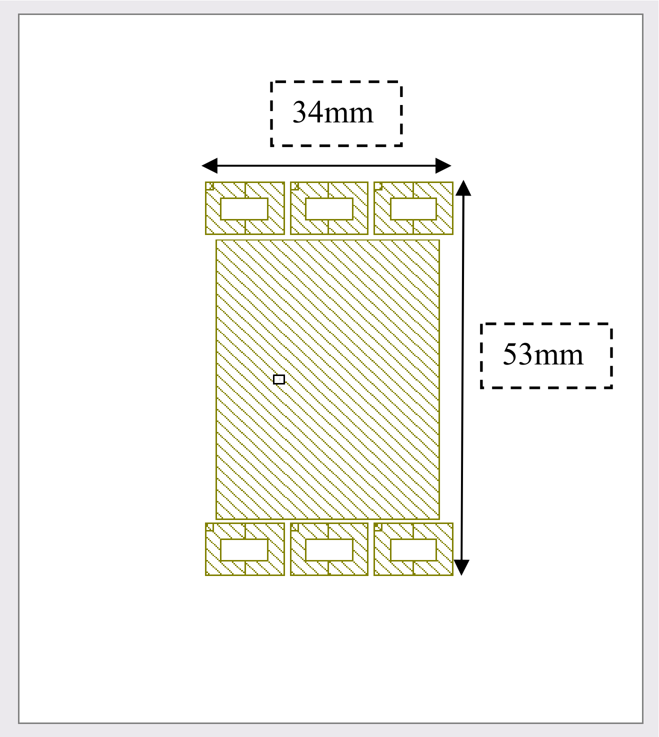

Figure 5.15: EM structure of microstrip antenna with EBG structure.

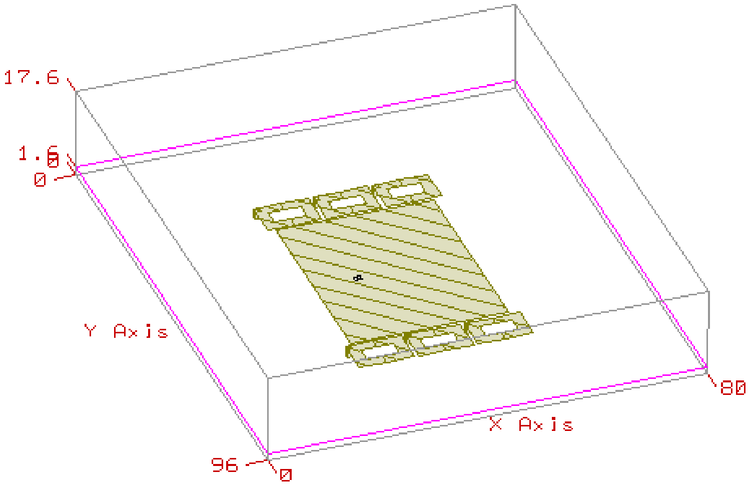

Figure 5.16:3D layout of the microstrip antenna with EBG structure.

Figure 5.17 shows the maximum radiation at 0° and the gain is 7.689dB. The same elevation for Etheta = 0° and Ephi = 90° are measured for comparison purposes.

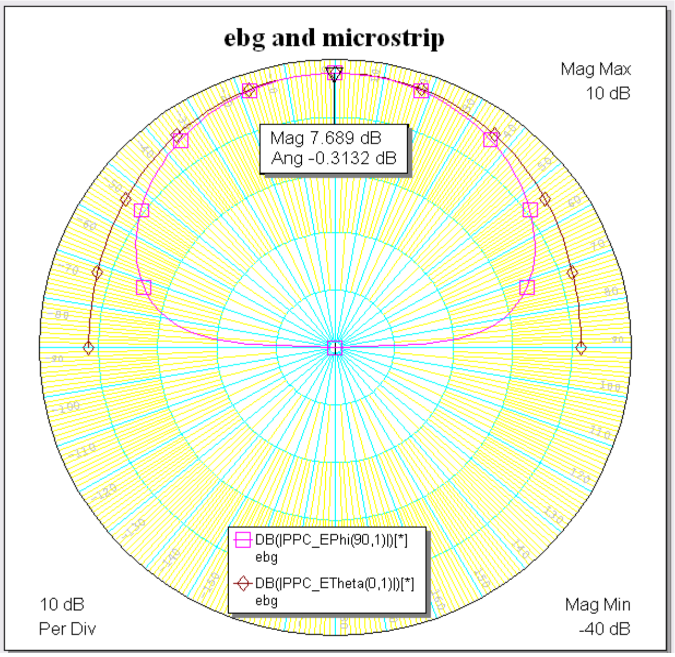

Figure 5.17: Maximum radiation at 0°, gain = 7.689dB for microstrip antenna with EBG structure.

Table 5.1: Comparison between conventional microstrip antenna and microstrip antenna with EBG structure.

	Conventional microstrip antenna	Microstrip antenna with EBG structure
Maximum radiation gain at 0°	5.58dB	7.689dB

5.4 Summary

This chapter provides the simulation and measured results for the three designed discussed in chapter 4. The first design is the conventional microstrip antenna, followed by the new EBG structure and the combination of both two in order to improve the performance of the microstrip antenna.

For conventional microstrip antenna, the Return Loss (RL), bandwidth and the maximum radiation pattern value were observed. With the dimension of 28.6mm versus

37.7mm, it is found that the RL is -20.68dB at 2.4GHz with 2.2% of bandwidth and maximum radiation gain of 5.58dB.

The new EBG designed is proved to operate at 2.4GHz. The simulation of the structure involves the parametric study of position of vias and the separation (gap) distance of the single unit of the EBG structure.

The final design is the microstrip antenna with EBG structure. The main result is the comparison of the maximum radiation gain. Its shows that the microstrip antenna with EBG structure produces gain of 7.689dB compared with 5.58dB for the microstrip antenna alone.

CHAPTER 6

CONCLUSIONS AND SUGGESTIONS

6.1 Conclusion

The goals of this project are to design a new EBG structure that can operate at 2.4GHz frequency and improve the performance of microstrip antenna when EBG structure added on it.

The conventional microstrip antenna was designed as a reference with the length of the patch is 28.6mm and the width of the patch is 37.7mm with a coaxial probe as a feed. The S11 (input return loss) plot for microstrip antennas have a magnitude of much less that –10dB at the operating frequency 2.4GHz, which means that the antennas had not many losses while transmitting the signal. The conventional patch simulation result gives the RL of –20.68dB. The gain of the radiation pattern was at 5.579dB.

The new EBG structure was designed using parametric studies and the best structure that can operate at 2.4GHz frequency is with of 34mm (width, W) x 35mm (length, L) with the single rectangular box of 10mm (width, W) x 7mm (length, L) and the vias with 1mm in diameter at the top left hand corner of the rectangular box structure. The S21 was simulated and measured to verify the stop band frequency of 2.4GHz.

It is proved that the microstrip antenna with EBG structure can improves the performance of the antenna. The maximum radiation pattern comparison of the conventional microstrip antenna versus microstrip antenna with EBG structure is measured to be 5.68dB compared with 7.689dB.

6.2 Suggestion for future works

A rectangular microstrip antenna with EBG structure was successfully designed to operate at 2.4GHz frequency with improvement in the maximum radiation pattern.

In the future, investigation into designing the microstrip antenna with different patch shapes and sizes are vital. In term of EBG structure, the design can be further improve with different in terms of basic parameters such as type of substrate, dielectric constant, the thickness of the substrate. From this project results also, we can design the EBG structure for different frequency of operation and even for multiband frequency.

The EBG structure also can be best applied in the array antenna to reduce the mutual coupling. This array antenna can be further classified according to the different thickness of the substrate and the various value of dielectric constant.

APPENDIX

PARAMETRIC STUDIES

1)

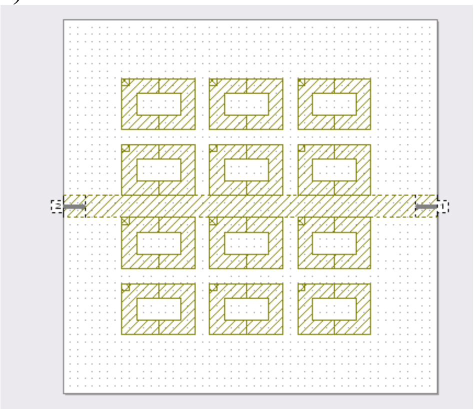

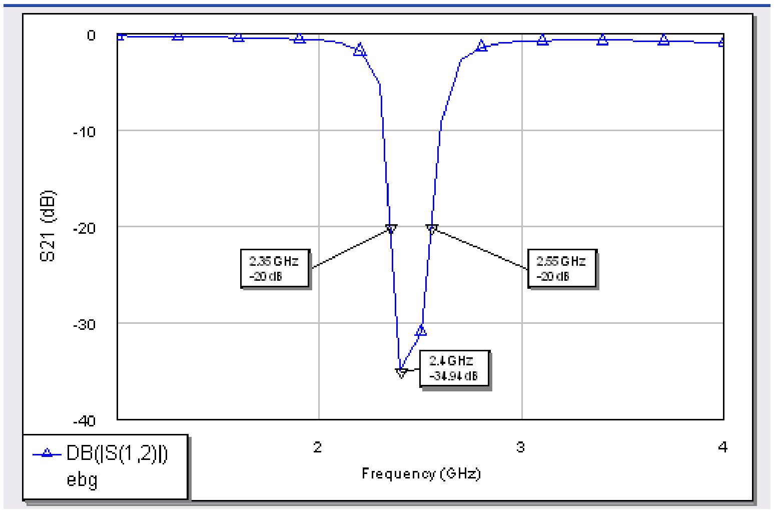

BW = 8.17%

2)

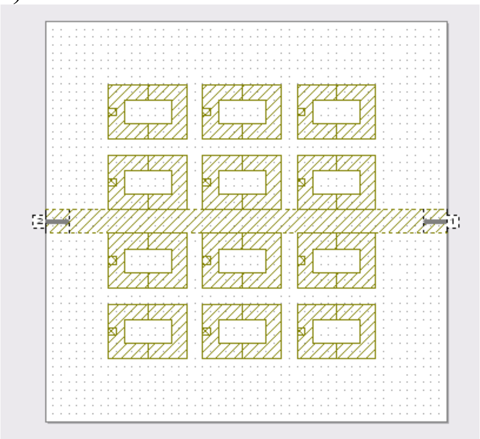

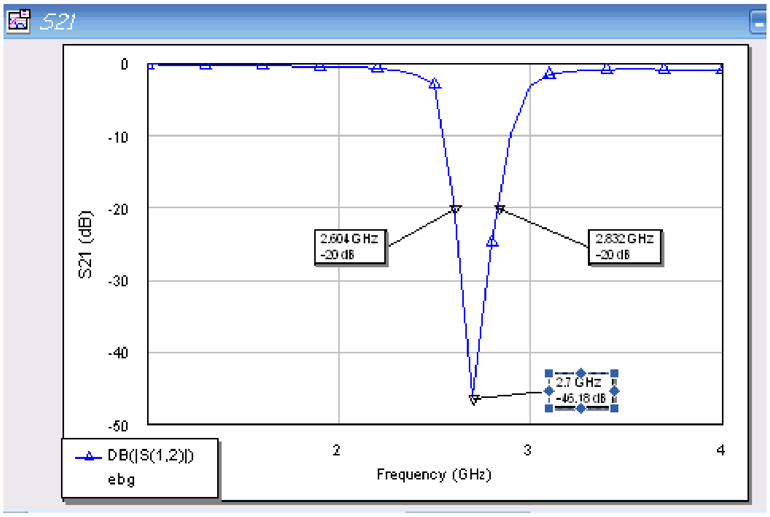

S21
0
-10
-20
-30
-40
-50
S21 (dB)
2.604 GHz
-20 dB
2.832 GHz
-20 dB
2.7 GHz
-46.18 dB
2
3
4
Frequency (GHz)
DB(|S(1,2)|)
ebg

BW= 8.30 %

3)

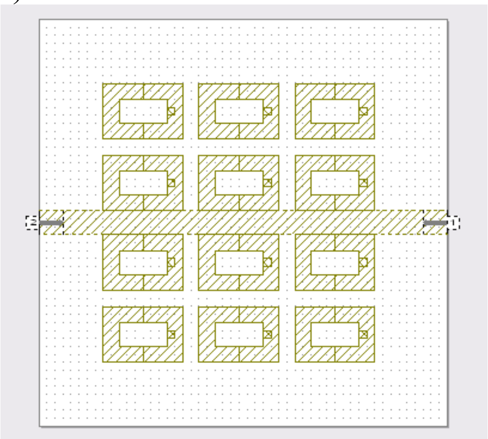

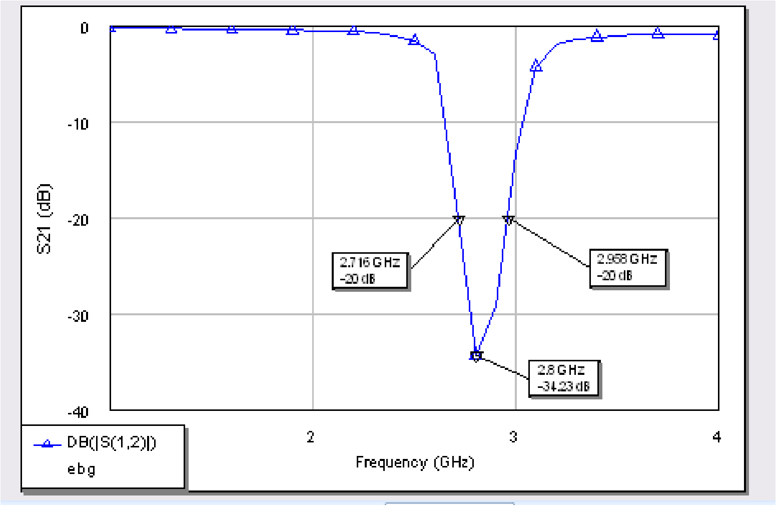
0
-10
-20
-30
-40
S21 (dB)
2.716 GHz
-20 dB
2.958 GHz
-20 dB
2.8 GHz
-34.23 dB
DB(|S(1,2)|)
ebg
2
3
4
Frequency (GHz)

BW = 8.54%

4)

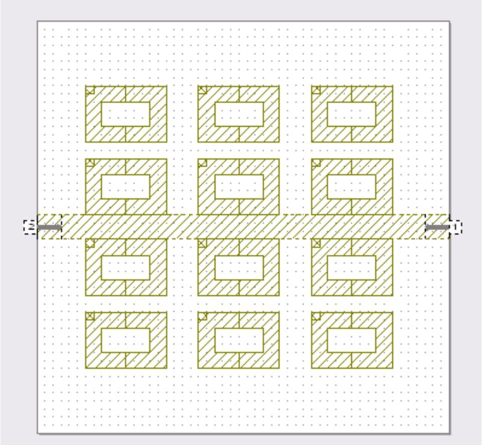

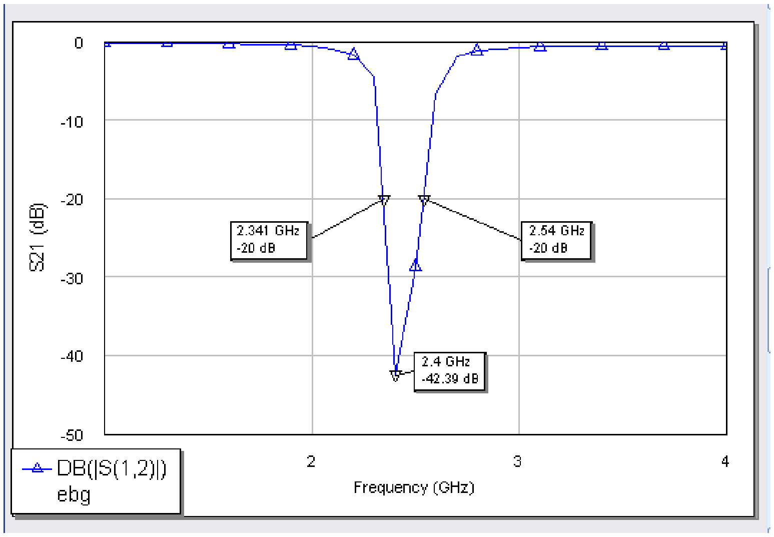
0
-10
-20
-30
-40
-50
S21 (dB)
2.341 GHz
-20 dB
2.54 GHz
-20 dB
2.4 GHz
-42.39 dB
DB(|S(1,2)|)
ebg
2
3
4
Frequency (GHz)

BW = 8.16%

5)

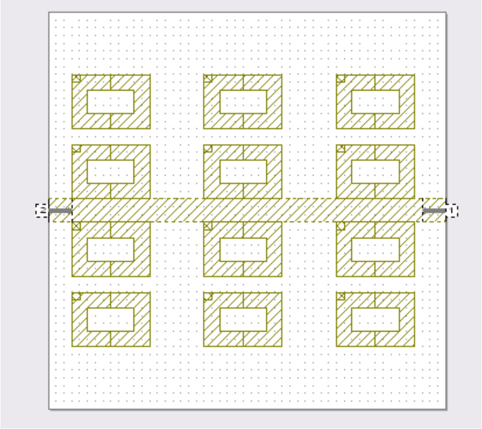

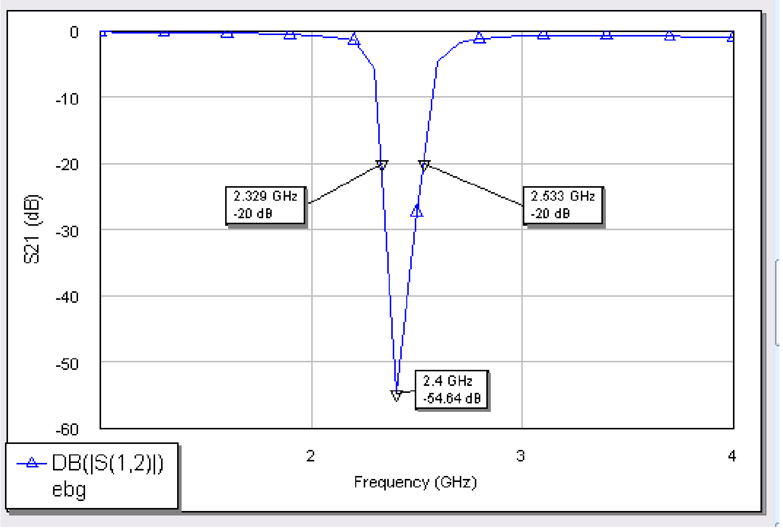
0
-10
-20
-30
-40
-50
-60
S21 (dB)
2.329 GHz
-20 dB
2.533 GHz
-20 dB
2.4 GHz
-54.64 dB
2
3
4
Frequency (GHz)
DB(|S(1,2)|)
ebg

BW = 8.39%

6)

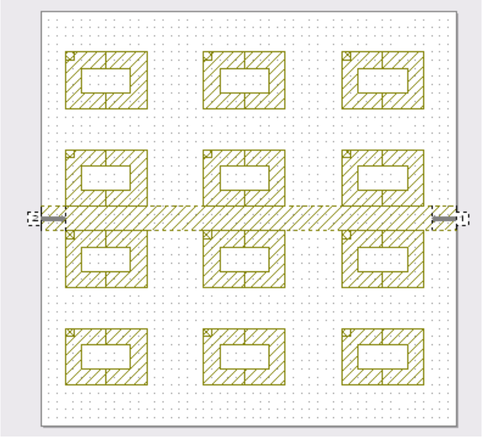

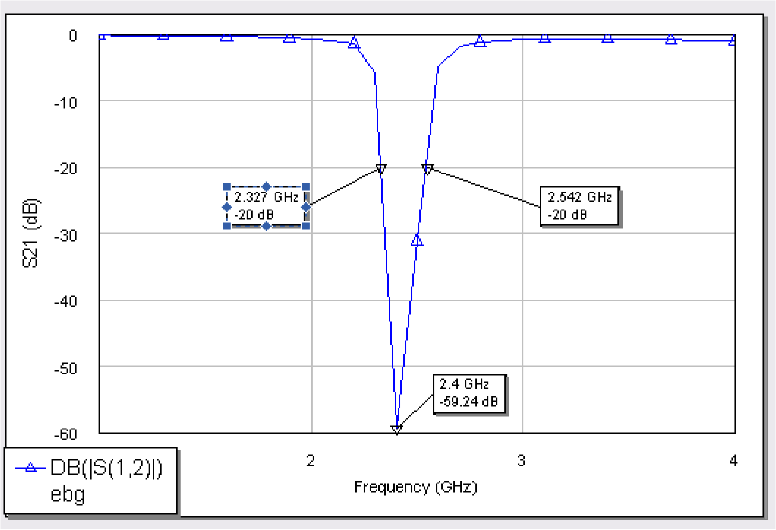
0
-10
-20
-30
-40
-50
-60
S21 (dB)
2.327 GHz
-20 dB
2.542 GHz
-20 dB
2.4 GHz
-59.24 dB
2
3
4
Frequency (GHz)
DB(|S(1,2)|)
ebg

BW = 8.84%

7)

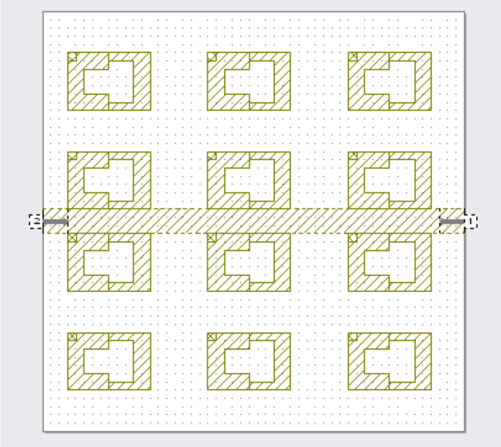

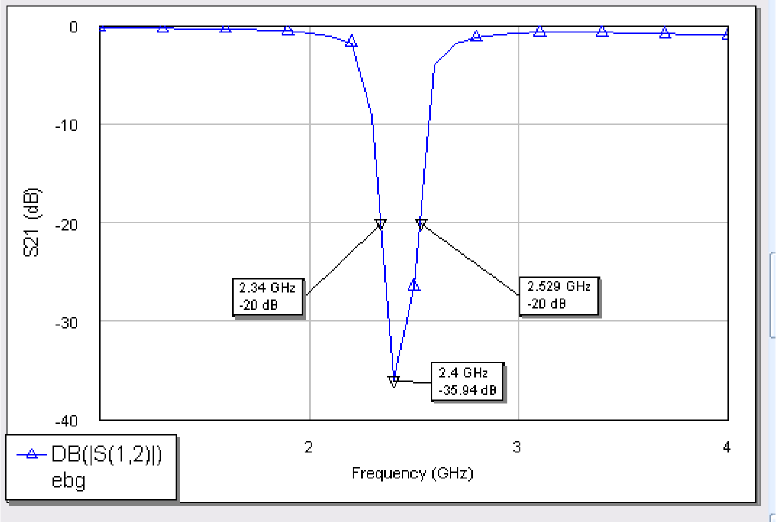
0
-10
-20
-30
-40
S21 (dB)
2
3
4
Frequency (GHz)
2.34 GHz
-20 dB
2.529 GHz
-20 dB
2.4 GHz
-35.94 dB
DB(|S(1,2)|)
ebg

8)

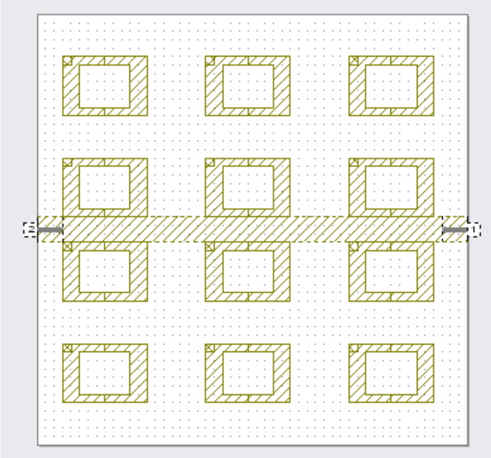

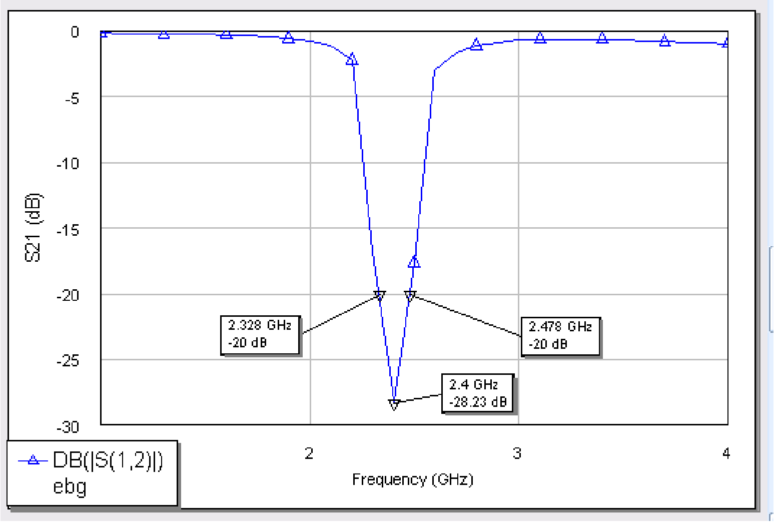
0
-5
-10
-15
-20
-25
-30
S21 (dB)
2
3
4
Frequency (GHz)
2.328 GHz
-20 dB
2.478 GHz
-20 dB
2.4 GHz
-28.23 dB
DB(|S(1,2)|)
ebg

E-plane

1) Satu (separation = $\lambda/2$)

Mag = 9.018dB Ang = 0.1184dB

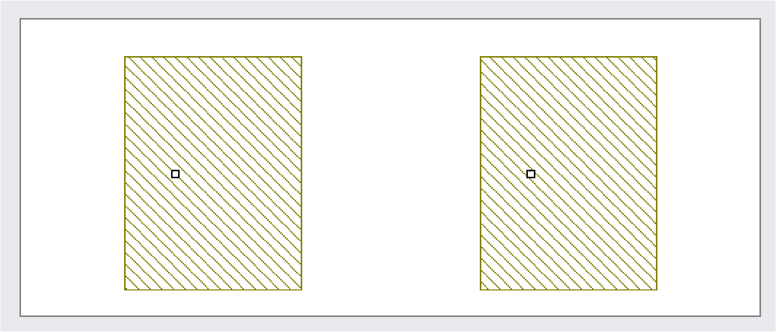

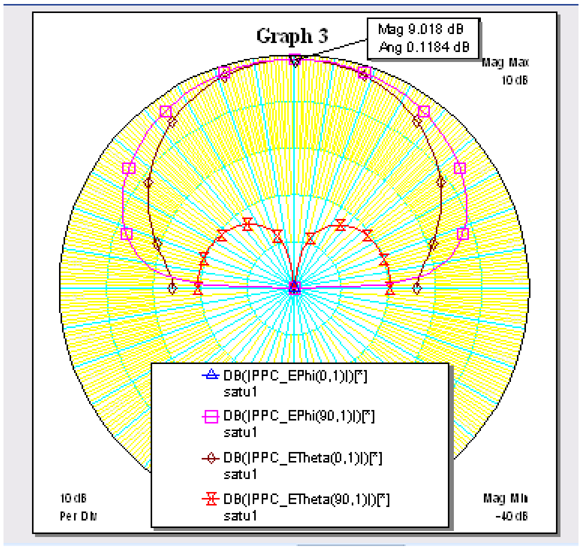

2) Satua (separation = λ/2 + ebg)

Mag = 9.016dB Ang = 0.1249

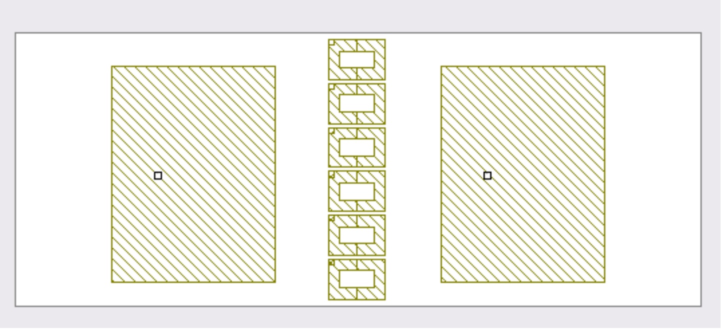

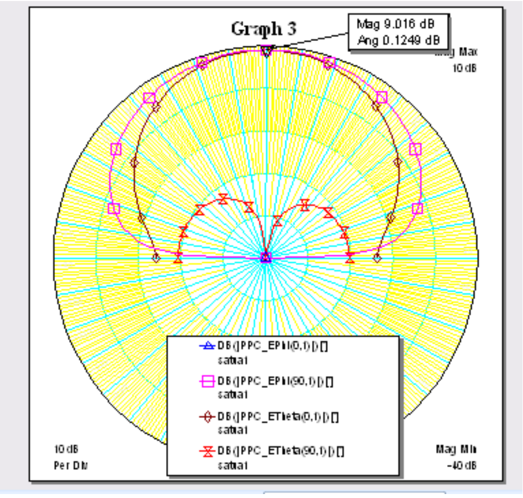

3) Dua (separation = λ/4)

Mag = 8.53dB Ang = 0.8101dB

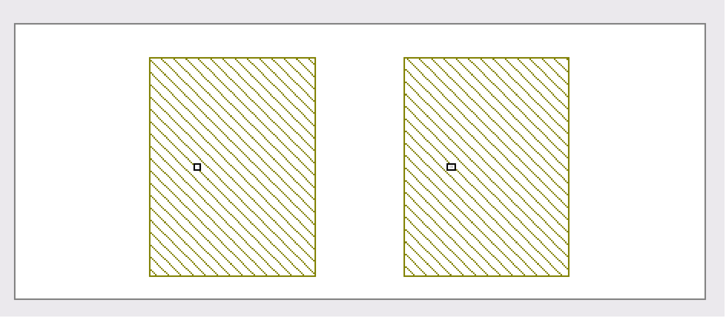

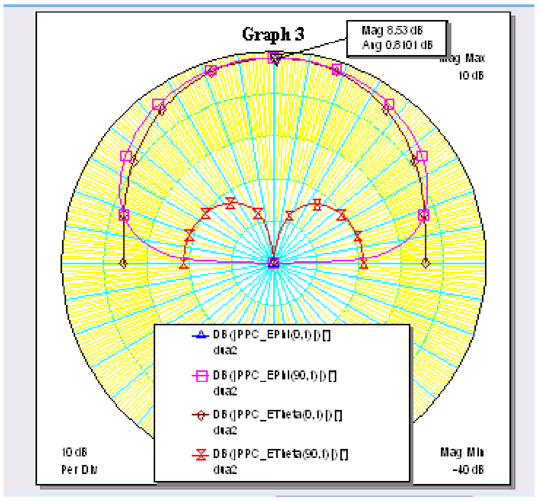

4) Duaa (separation = λ/4 + ebg)

Mag = 8.519dB   Ang = 0.5013dB

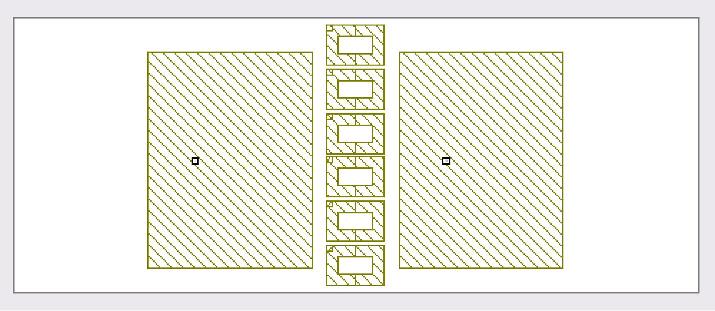

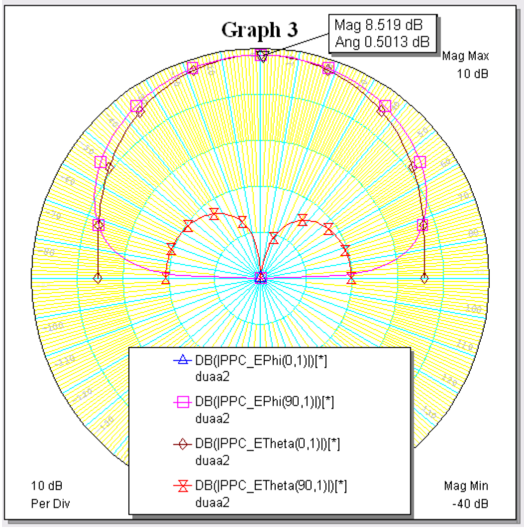

5) Duab (small separation + ebg)

Mag = 8.17dB Ang = 0.8419dB

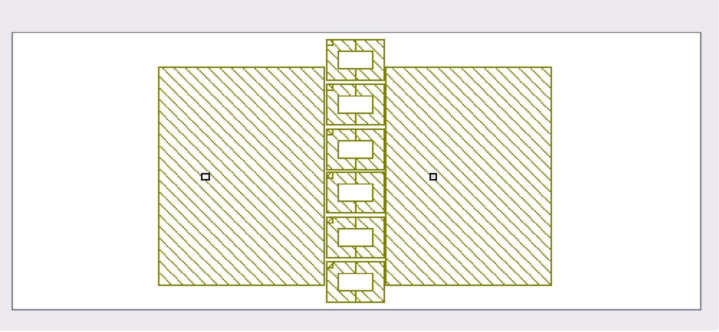

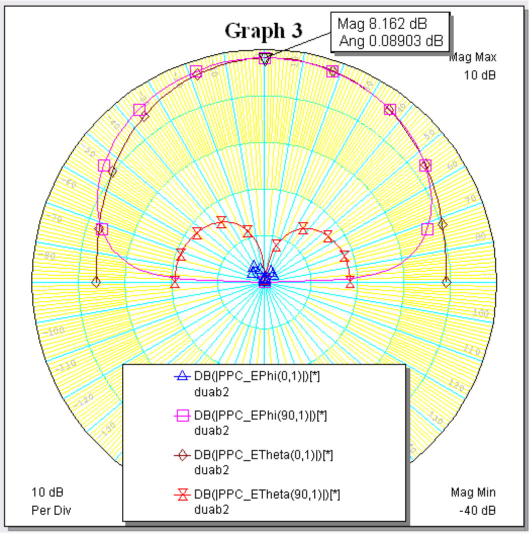

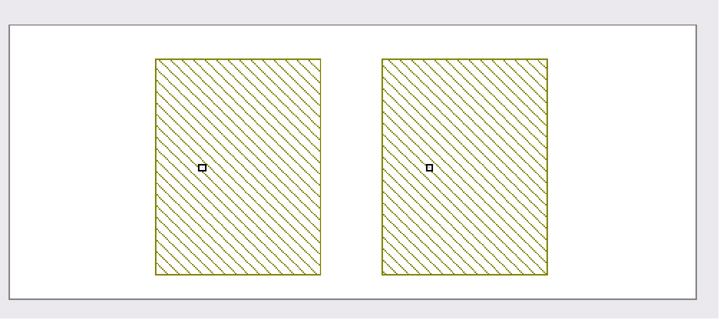

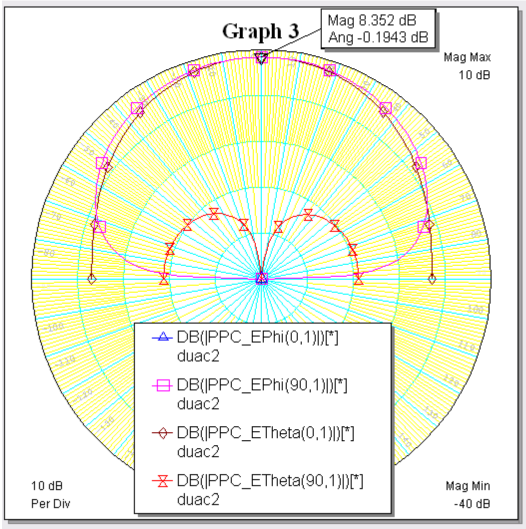
Graph 3
Mag 8.352 dB
Ang -0.1943 dB
Mag Max
10 dB
10 dB
Per Div
Mag Min
-40 dB
DB(|PPC_EPhi(0,1)|)[*]
duac2
DB(|PPC_EPhi(90,1)|)[*]
duac2
DB(|PPC_ETheta(0,1)|)[*]
duac2
DB(|PPC_ETheta(90,1)|)[*]
duac2

H-plane

6) Tiga (separation = λ/2)

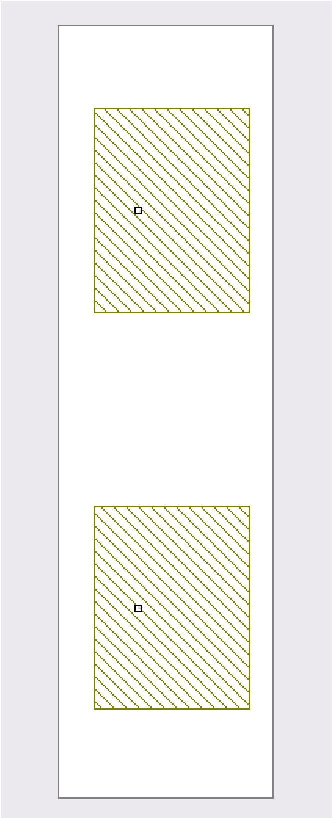

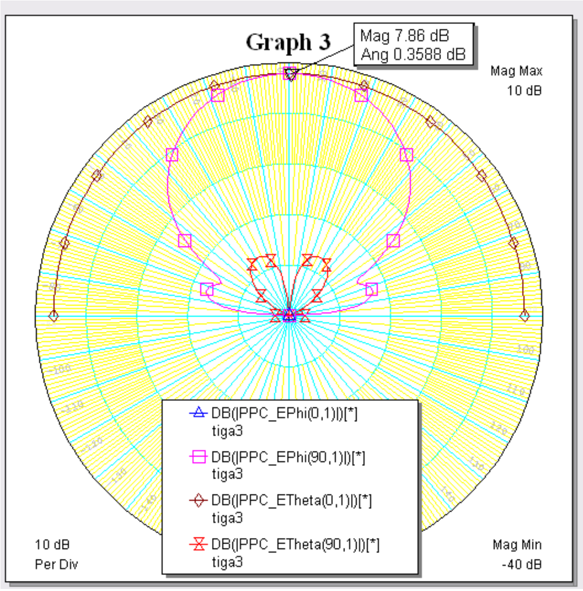

7) Tigaa (separation = λ/2 + ebg)

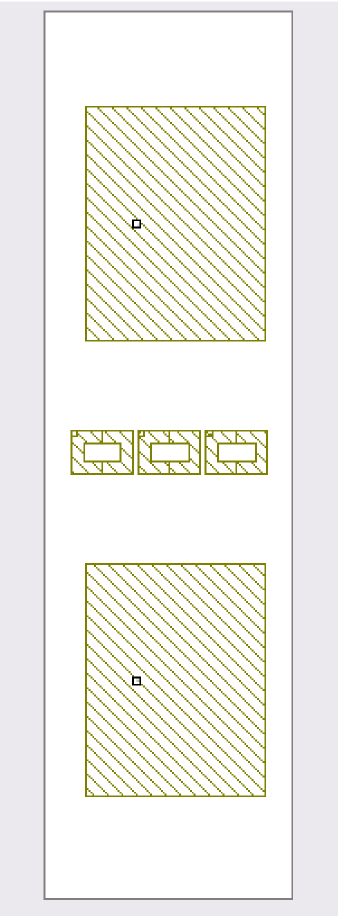

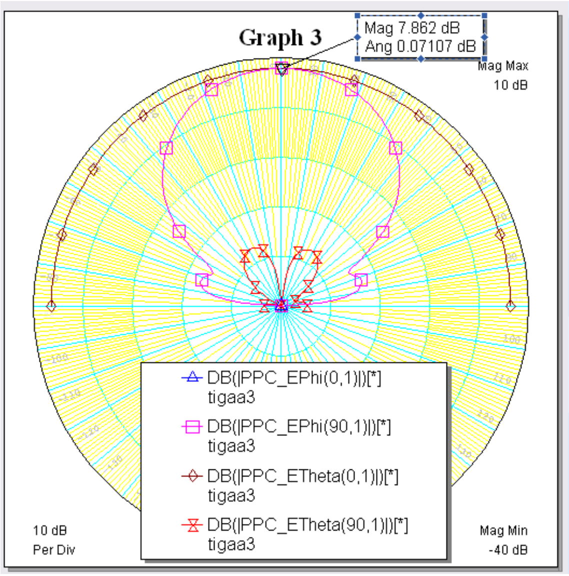

8) Empat (separation = λ/4)

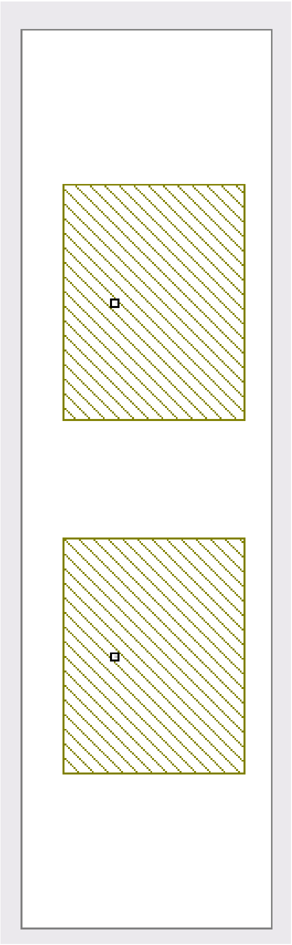

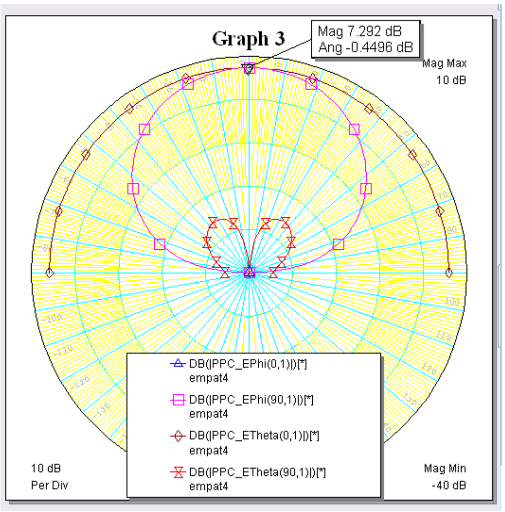

9) Empata (separation = λ/4 + ebg)

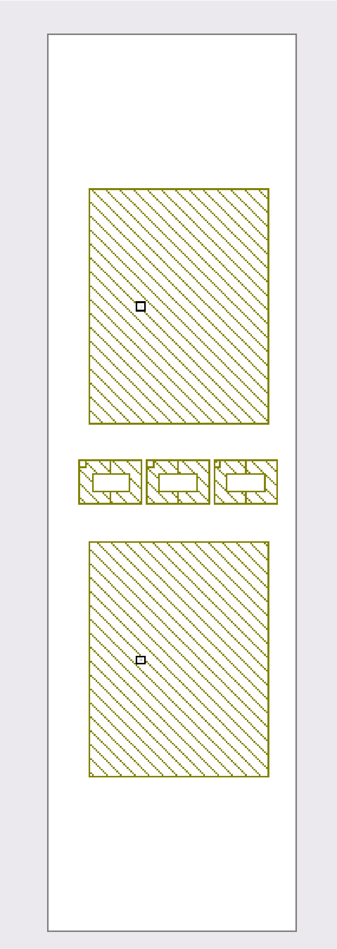

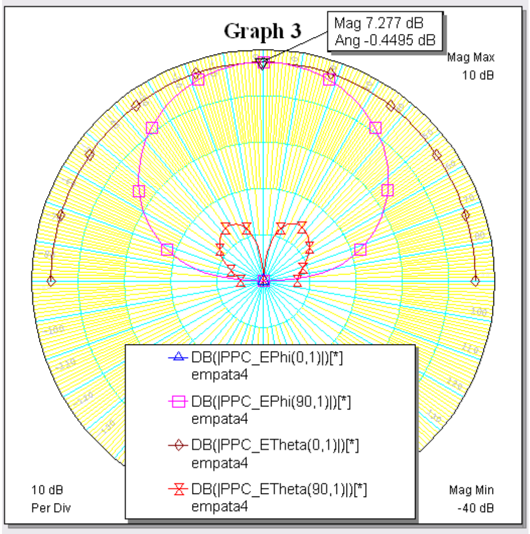

10) Rr

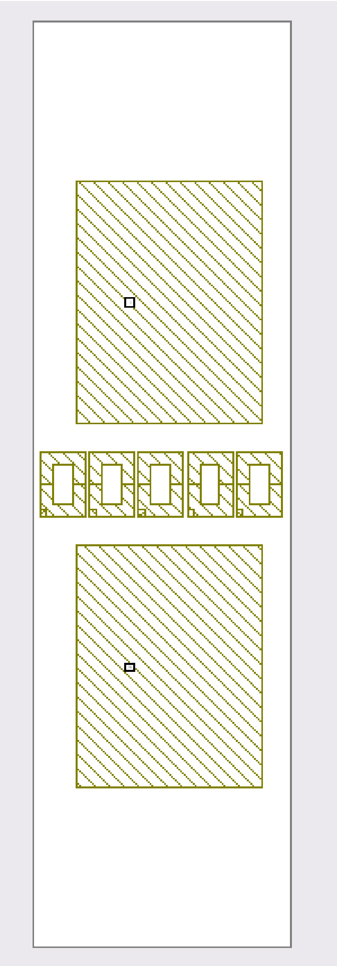

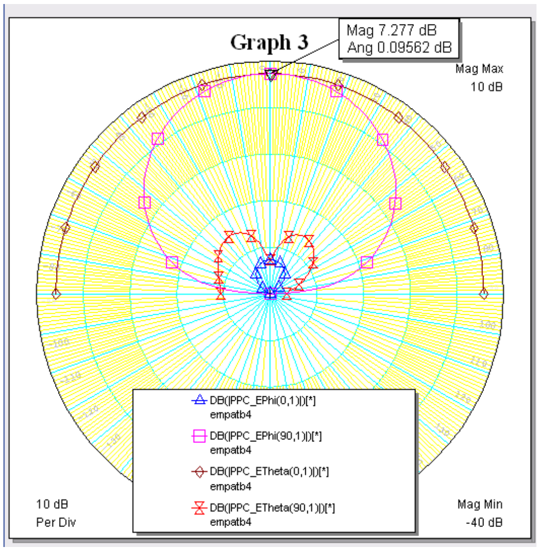
Graph 3
Mag 7.277 dB
Ang 0.09562 dB
Mag Max
10 dB
DB(|PPC_EPhi(0,1)|)[*]
empatb4
DB(|PPC_EPhi(90,1)|)[*]
empatb4
DB(|PPC_ETheta(0,1)|)[*]
empatb4
DB(|PPC_ETheta(90,1)|)[*]
empatb4
10 dB
Per Div
Mag Min
-40 dB

11)

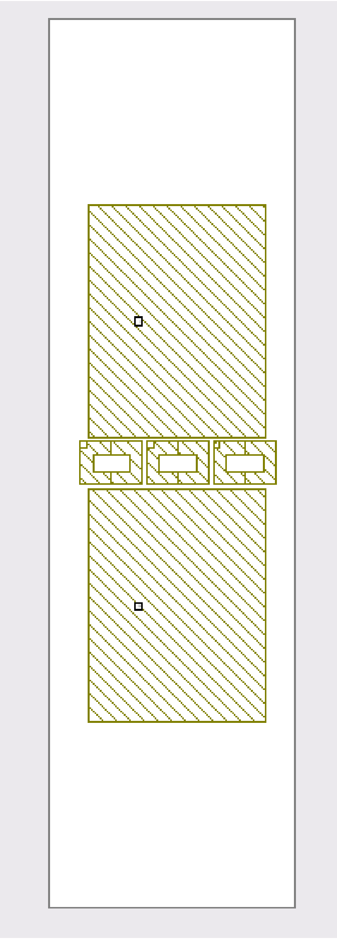

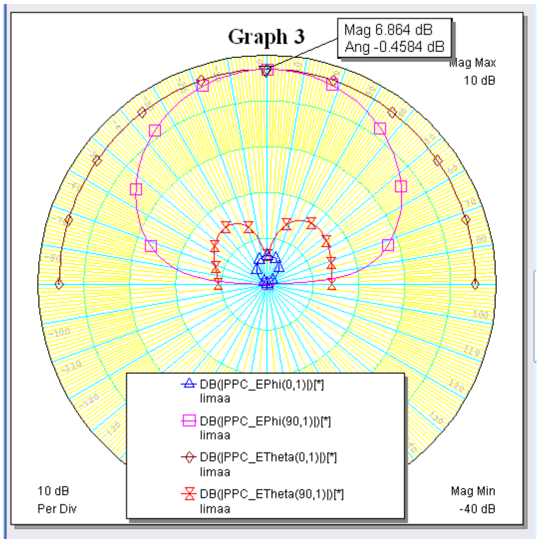
Graph 3
Mag 6.864 dB
Ang -0.4584 dB
Mag Max
10 dB
DB(|PPC_EPhi(0,1)|)[*]
limaa
DB(|PPC_EPhi(90,1)|)[*]
limaa
DB(|PPC_ETheta(0,1)|)[*]
limaa
DB(|PPC_ETheta(90,1)|)[*]
limaa
10 dB
Per Div
Mag Min
-40 dB

12) Tt

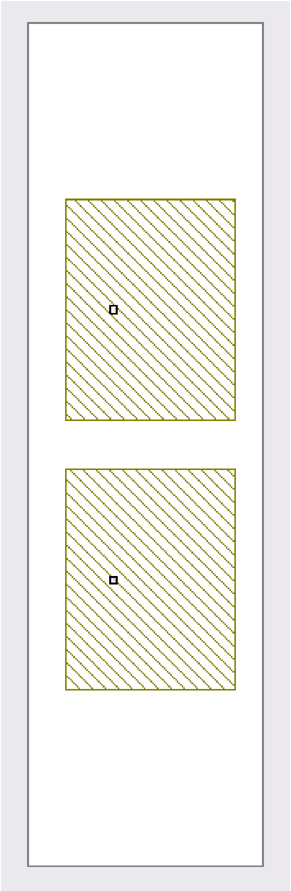

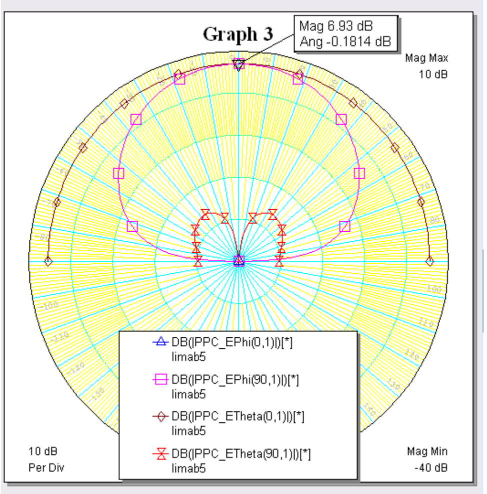
Graph 3
Mag 6.93 dB
Ang -0.1814 dB
Mag Max
10 dB
10 dB
Per Div
Mag Min
-40 dB
DB(|PPC_EPhi(0,1)|)[*]
limab5
DB(|PPC_EPhi(90,1)|)[*]
limab5
DB(|PPC_ETheta(0,1)|)[*]
limab5
DB(|PPC_ETheta(90,1)|)[*]
limab5

EBG

1)

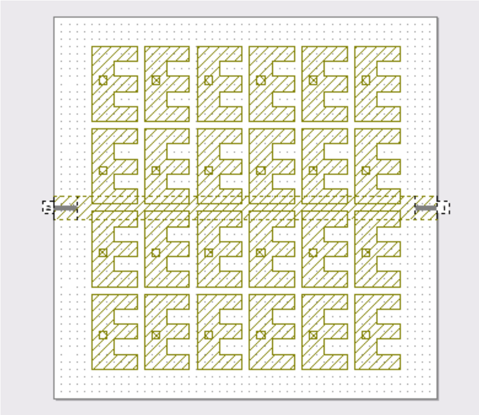

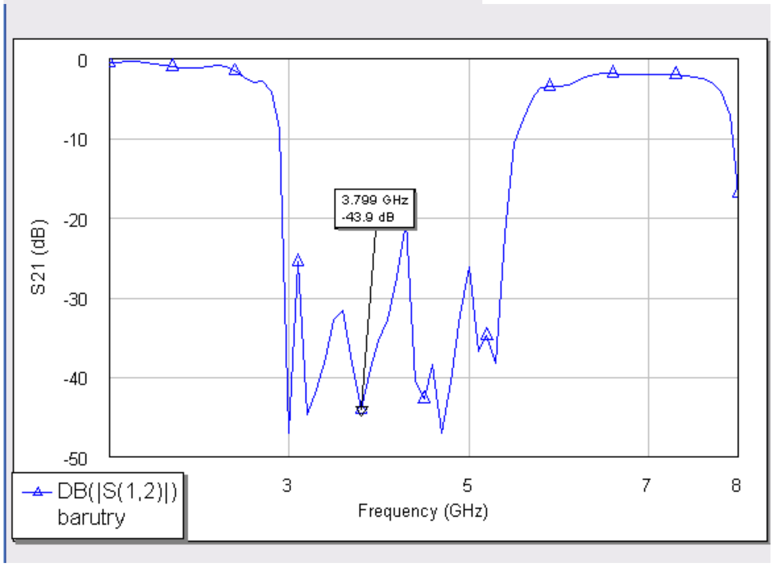
0
-10
-20
-30
-40
-50
S21 (dB)
3.799 GHz
-43.9 dB
3
5
7
8
Frequency (GHz)
DB(|S(1,2)|)
barutry

2)

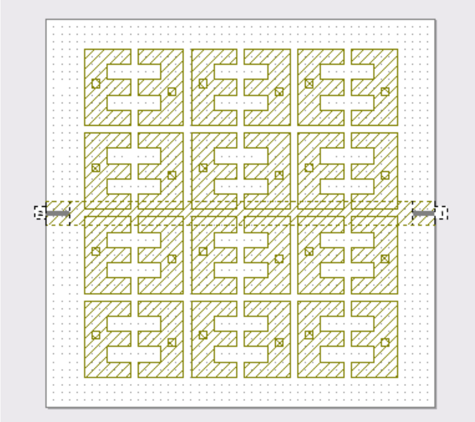

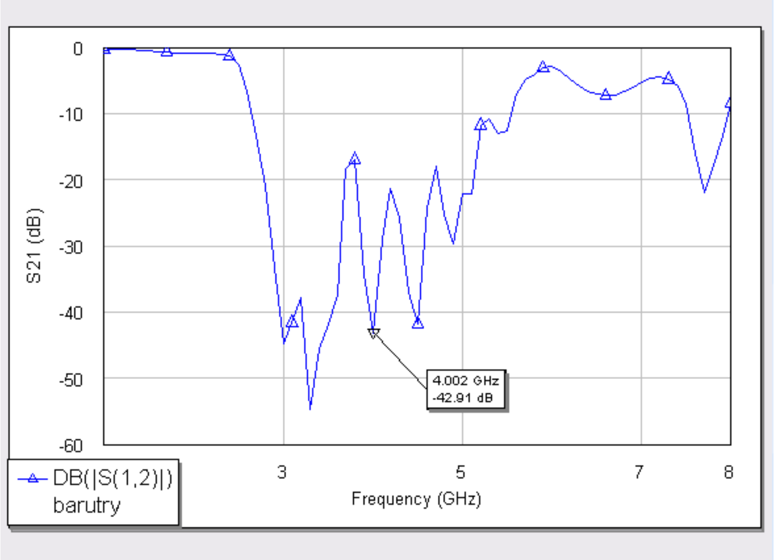
0
-10
-20
-30
-40
-50
-60
S21 (dB)
3
5
7
8
Frequency (GHz)
4.002 GHz
-42.91 dB
DB(|S(1,2)|)
barutry

3)

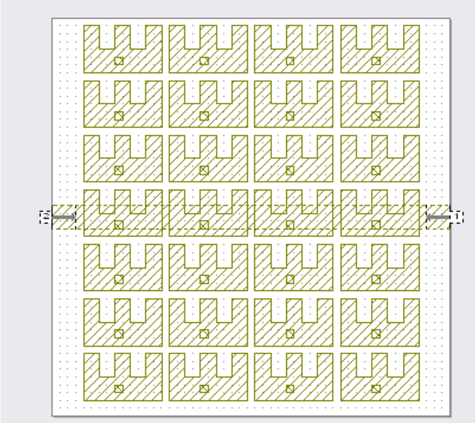

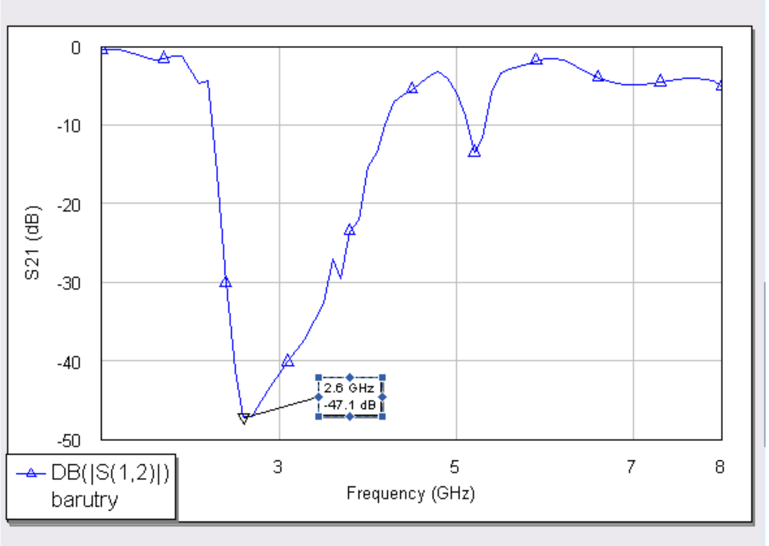
0
-10
-20
-30
-40
-50
S21 (dB)
2.6 GHz
-47.1 dB
3
5
7
8
Frequency (GHz)
DB(|S(1,2)|)
barutry

4)

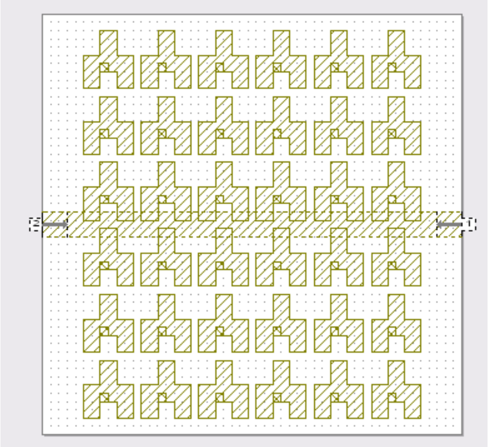

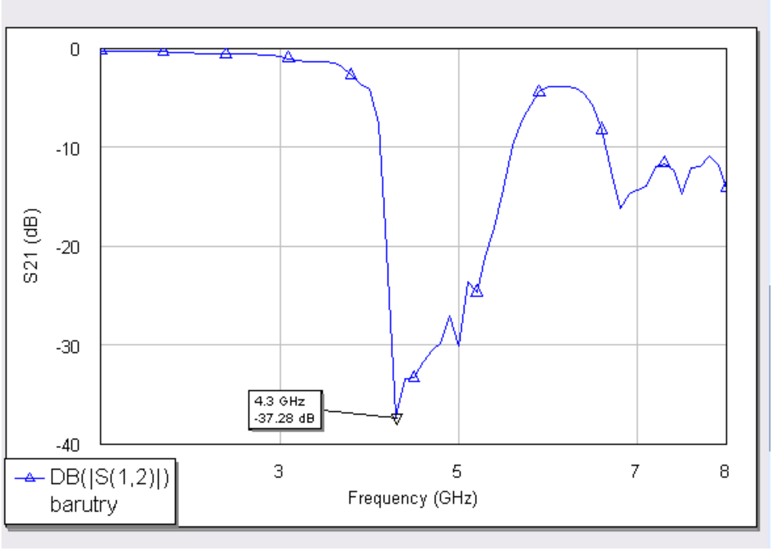
0
-10
-20
-30
-40
S21 (dB)
4.3 GHz
-37.28 dB
3
5
7
8
Frequency (GHz)
DB(|S(1,2)|)
barutry